Minerals Engineering 170 (2021) 107004

Contents lists available at ScienceDirect

Minerals Engineering

journal homepage: www.elsevier.com/locate/mineng

New perspectives in iron ore flotation: Use of collector reagents without depressants in reverse cationic flotation of quartz

Klaydison Silva [a,b], Lev O. Filippov [a,*], Alexandre Piçarra [a], Inna V. Flilippova [a], Neymayer Lima [b], Anna Skliar [a], Lívia Faustino [c,d], Laurindo Leal Filho [d]

[a] Université de Lorraine, CNRS, GeoRessources, F54000 Nancy, France
[b] Vale Mining Company, Iron Ore Beneficiation Development Team, Minas Gerais, Brazil
[c] Vale Institute of Technology, Minas Gerais, Brazil
[d] University of São Paulo – USP, São Paulo, Brazil

ARTICLE INFO

Keywords:
Iron ore
Flotation
Amidoamine
Quartz
Kaolinite
Hematite

ABSTRACT

The reverse flotation of the iron ore with etheramine collector is significantly impacted when the iron-bearing silicates and the kaolinite are present in the silicates gangue mineral complex. This paper aims to propose a new amidoamine collector N-[3-(Dimethylamino)propyl]dodecanamide for iron ore reverse flotation with a potential of removing the iron oxides depressant. The contact angle and electrophoretic mobility measurements as well as the flotation experiments were performed on the pure quartz, kaolinite and hematite samples to compare its effect with the etheramine which is widely used as collector in reverse flotation of iron ores. Infrared spectroscopy was performed to study the adsorption of the amidoamine collector on the surface of the minerals studied.

Amidoamine collector showed a significant selectivity towards quartz while the flotation of hematite and kaolinite were inhibited at pH 10 without the presence of a depressor. A total floatability of quartz was explained by increased contact angle from 10° to about 50° without impacting significantly the contact angle measured on the hematite (9.4° to 17°). Surface hindrance effect caused by the structure of the N-[3-(Dimethylamino)propyl] dodecanamide collector on the hematite surface is the most suitable hypothesis concerning the high selectivity regarding the iron ore reverse flotation process.

1. Introduction

The flotation processes performed in the main iron ore beneficiation plants located in the Iron Quadrangle region (Brazil) consist of flotation of natural fine particles (below 0.15 mm, without grinding) or flotation of all the material after grinding using ball mills (run of mine). In both cases, the flotation process adopted is a reverse cationic process with a preliminary desliming stage of flotation feed to remove materials with particle sizes below 10 μm (slimes) that are harmful to the iron ore flotation process (Filippov et al., 2014).

The reverse cationic flotation is also largely used to reduce the silica content in the iron concentrate obtained through magnetic separation. It is the most efficient upgrading process for simple systems composed of hematite/magnetite and quartz (Araujo et al., 2005; Filippov et al., 2014). However, its separation efficiency decreases when as a part of the gangue minerals there are Fe/Mg silicates. These Fe/Mg bearing gangue minerals cause a reduction in the flotation efficiency because their surface properties are similar to those of iron oxides, resulting in the non-selective action of depressants such as starch (Filippov et al., 2010; 2013).

Studies performed on the flotation of quartz with etheramines as collectors showed the efficient depression of iron oxides by starch molecules from different sources (such as corn and potato) (Araujo et al., 2005; Kar et al., 2013). However, detailed studies on reverse cationic flotation with iron ore samples from different deposits over the world (Brazil, Russia, Mexico) performed by Filippov and co-workers confirmed the inefficiency of starch when the silica content in the concentrate is controlled by Fe/Mgbearing minerals such as amphiboles, epidote, chamosite, and diopside (Filippov et al., 2010; Severov et al., 2016; Veloso et al., 2018). The main approaches for solving these issues focus on using new collector formulations (Filippov et al., 2010) or new alternative depressants such as guar gum (Turrer and Peres, 2010),

* Corresponding author.
E-mail address: lev.filippov@univ-lorraine.fr (L.O. Filippov).

https://doi.org/10.1016/j.mineng.2021.107004
Received 11 August 2020; Received in revised form 27 May 2021; Accepted 1 June 2021
Available online 14 June 2021

humic acid (Dos Santos and Oliveira, 2007; Veloso et al., 2018), lignosulfonate, and carboxymethyl cellulose (Turrer and Peres, 2010; Veloso et al., 2020), leading to better flotation selectivity between hematite and silicates. However, the alternative depressants tested inhibited flotation of quartz owing to physical adsorption on their surfaces (Turrer and Peres, 2010). Based on Fourier transform infrared (FTIR) spectroscopy data, Severov et al., (2013) showed that starch can also adsorb on the quartz surface owing to the formation of hydrogen bonds between the hydroxyl groups of the polysaccharides and silanol groups presents on the quartz surface at pH 10. Direct adsorption studies confirmed similar adsorption densities on the surfaces of Fe-bearing silicates (pargasite) and quartz, with magnetite also showing high adsorption density (Filippov et al., 2013). However, starch adsorption on quartz and hematite is different not merely in terms of magnitude but also in bonding strength. This is because the adsorption of the polysaccharides on the iron oxides and Fe-bearing silicates is controlled by their chemical bonding with the iron in the mineral structure (Weissenborn et al., 1995; Filippov et al., 2013); however, hydrogen bonding is the main adsorption mechanism on the quartz surface. Thus, amine collectors can replace the starch molecules on the quartz surface because of their stronger electrostatic interactions with the negatively charged quartz surface supported by lateral chain–chain interactions. Strong interactions of starch and other depressants on the Fe-bearing mineral surface through covalent bonding between the iron atoms and hydroxyl groups of the depressants lead to increased hydrophilic behaviour of such silicates when amines are used as flotation collectors. Hence, the investigations on new flotation collectors can contribute toward unlocking new iron ore resources related to primary deposits with complex gangue mineralogy (i.e., Fe-bearing silicates, kaolinite) or processing of old tailings with high degrees of alterations.

Amidoamine collectors were suggested and tested as effective agents for the flotation process, with diethylenetriamine monoamide being the most commonly used (Friedli, 1990). This type of reagent is obtained by the reaction between polyamines and organic acids. Amidoamines provide several advantages for the flotation process, i.e., selectivity and cost reduction (Friedli, 1990). In phosphate ore concentration processes, amidoamines are more tolerant toward sulphate ions. They are also inexpensive and have fewer complications due to possible overdosage (Friedli, 1990). There are very few studies reporting the use of amidoamine molecules in iron ore flotation. However, they can be efficient quartz collectors in conventional iron ore reverse flotation using starch as the depressant of iron oxides.

Amidoamine-based collectors are suitable candidates for developing efficient iron ore slime flotation processes. As reported in earlier studies, iron ore slimes are generally composed of other minerals in addition to iron oxides and quartz (Lima et al., 2020). Some slimes from the Iron Quadrangle in Brazil, for example, have considerable amounts of kaolinite in their composition.

The choice of reagent is not the only factor considered for developing an iron ore slime flotation processes. It is also necessary to determine the ideal hydrodynamic conditions for these processes (Fornasiero and Filippov, 2017). However, to determine the hydrodynamic conditions, it is first necessary to develop reagents that make the process viable. There are some shortcomings in the industrial flotation process with amine collectors. These shortcomings worsen the flotation indexes, resulting in low collectability, poor selectivity, large cohesive bubbles, and sensitivity to slime presence (Liu, et al., 2019).

In this study a comparison between a new amidoamine collector N-[3-(Dimethylamino)propyl]dodecanamide) with etheramine and oleate collectors in the flotation of pure minerals such as hematite, quartz and kaolinite is presented and discussed. The study was done with the focus on developing alternative routes that will allow the concentration of iron ore by flotation without a depressant reagent.

2. Materials and methods

2.1. Minerals and reagents

Pure quartz, kaolinite, and hematite mineral samples were used in this study. The kaolinite sample (Morbihan) was provided by Société Nouvelle d'Exploitation des Kaolins du Morbihan, the quartz sample was provided by Sibelco and the hematite sample was provided by Minerama.

The quartz and hematite samples were crushed using jaw and gyratory crushers. The size of hematite was reduced to flotation size (d90 = 100 μm) using a laboratory ball mill. To avoid surface contamination of the silicates, they were milled using a ceramic ball mill to obtain sizes below 100 μm. The size distributions of the mineral samples used for this study are presented in Fig. 1.

XRD analysis results show the purity of the obtained products (Fig. 2).

The flotation performance of three collectors (etheramine, oleate, and N-[3-(Dimethylamino)propyl]dodecanamide) was evaluated through kinetic flotation tests, performed with pure mineral samples of hematite, quartz, and kaolinite and mixtures of these minerals. From this point on, the collector N-[3-(Dimethylamino)propyl]dodecanamide will be referred to as "amidoamine".

Additionally, the reagents used are listed in Table 1.

2.2. X-Ray fluorescence (XRF) analysis

XRF analysis was performed by using a Thermo Fisher Scientific Niton XL3t XRF Analyser, with objective to analyse the percentage of elements in the products obtained during flotation. The measurements were performed using the four filters available in the analyser, with each filter operated for 30 s (total measurement time of 120 s) and the 'Cu-Zn' mode selected. For representative purposes, three measurements were performed for each sample.

Fig. 3 shows the correlation between the Fe contents determined via XRF (used in this work) and the inductively coupled plasma mass spectrometry (ICP-MS) results obtained by Service d'analyse des roches et des minéraux (SARM, Nancy, France), and the R^2 value obtained.

The R^2 value obtained (0.983) shows a satisfactory fit of the equation to transform Fe measurements by XRF into ICP-MS measurements. The XRF measurements have relatively small deviations from the ICP-MS results (roughly ± 0.5%). All the XRF measurements were corrected using the correlation equation given in Fig. 2.

2.3. Modified water

To simulate conditions similar to those in itabirite concentration plants in the Iron Quadrangle, mineral salts were mixed in the water. This modified water was used in the fundamental studies and flotation tests Table 2.

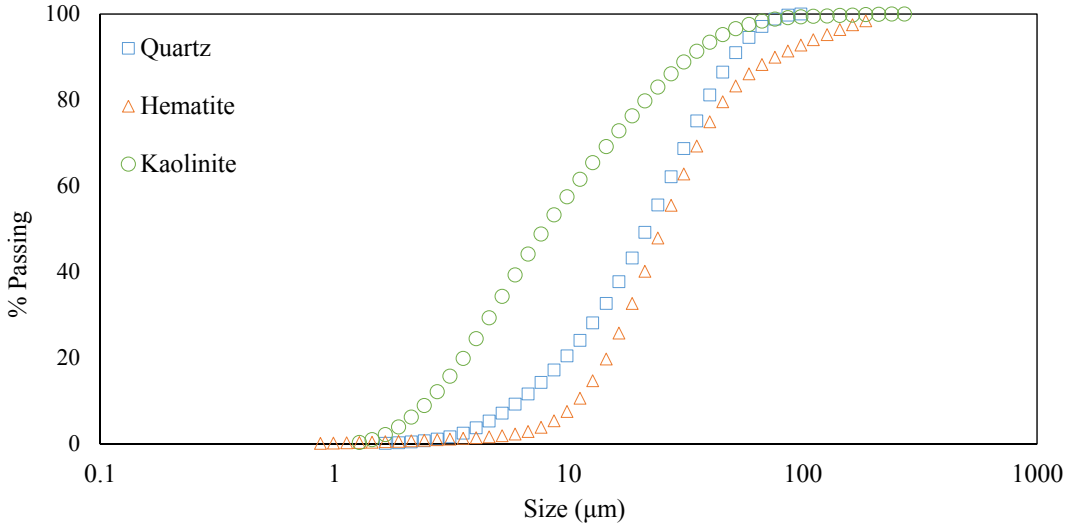

Fig. 1. Particle size distribution of pure mineral samples.

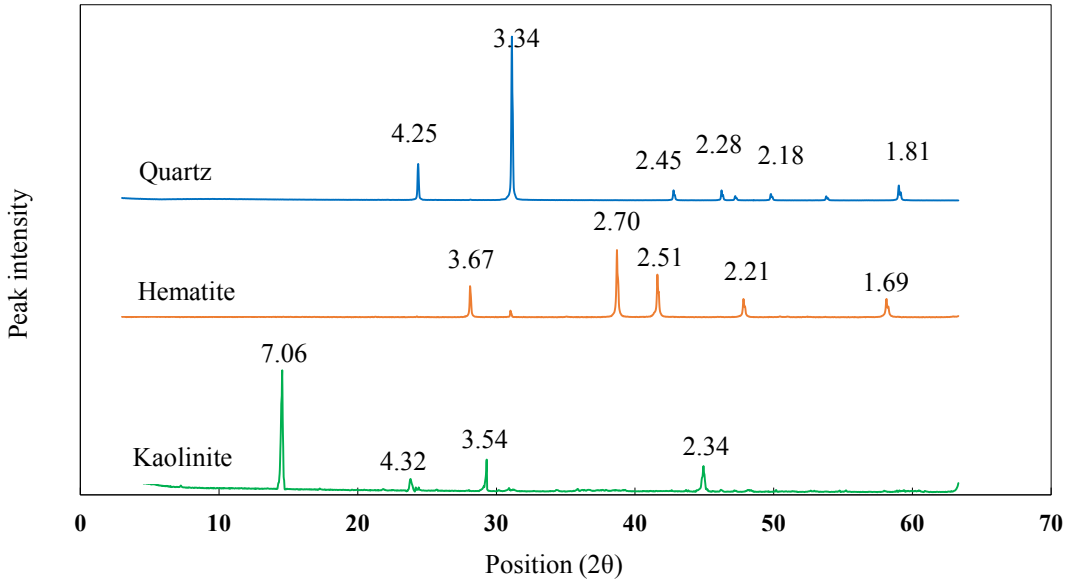

Fig. 2. XRD characterization of the hematite, quartz and kaolinite samples.

Table 1
Reagents used in the kinetic flotation tests.

Name	Role	Chemical formula	Provider
Corn starch	Depressant	$(C_6H_{10}O_5)n$	Sigma-Aldrich
Etheramine - Flotigam EDA	Collector	$R\text{-}O\text{-}C_2H_3\text{-}(NH_2)$	Clariant
Amidoamine - N-[3-(Dimethylamino)propyl]dodecanamide	Collector	$C_{17}H_{36}N_2O$	Clariant
Oleate - Oleic acid sodium salt	Collector	$C_{18}H_{33}NaO_2$	Roth
Sodium hydroxide	pH modifier	NaOH	Carlos Vela

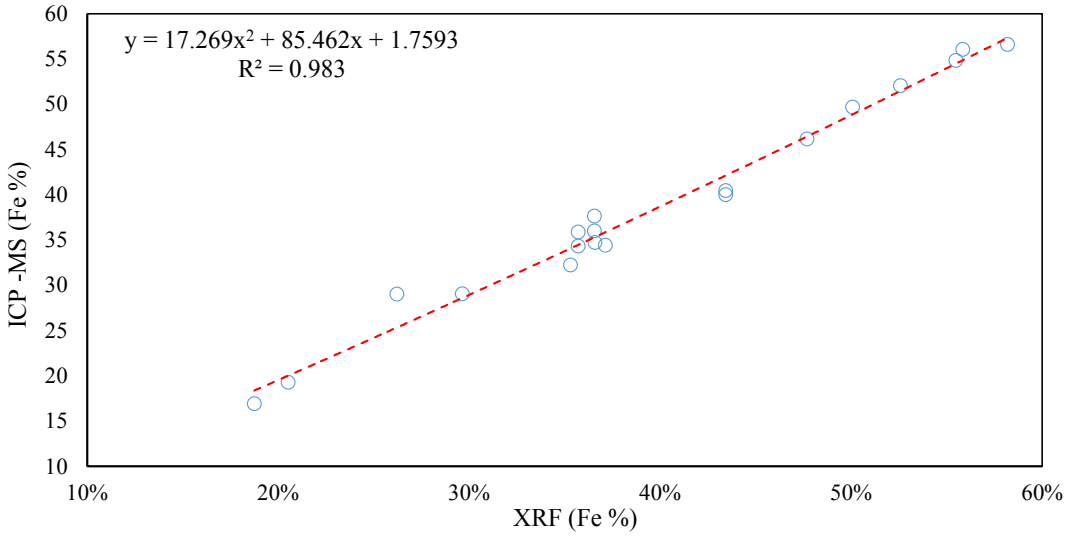

Fig. 3. Correlation between Fe contents determined via XRF and ICP-MS.

Table 2
Chemical analysis results of industrial water and salts used in the modified water.

Industrial process water		Modified water used in fundamentals studies	
Element	Concentration (g/L)	Salt used	Salt concentration (g/L)
Na	9.40×10^{-2}	Na_2SO_4	2.91×10^{-1}
K	1.01×10^{-3}	KCl	1.93×10^{-3}
Mn	1.42×10^{-4}	$MnSO_4{\cdot}H_2O$	4.36×10^{-4}
Al	1.12×10^{-4}	$Al_2(SO_4)_3{\cdot}18H_2O$	1.31×10^{-3}
Fe	1.39×10^{-3}	$FeCl_3{\cdot}6H_2O$	6.71×10^{-3}
Ca	1.16×10^{-4}	$CaCl_2{\cdot}2H_2O$	4.25×10^{-4}
$S/(SO_4)^{2-}$	9.21×10^{-2} / 1.22×10^{-1}	$(SO_4)^{2-}$	4.73×10^{-2}
Ionic strength (mol/L)	4.75×10^{-3}	Ionic strength (mol/L)	3.19×10^{-3}

2.4. Contact angle measurements

Contact angle measurements using a DSA25 Shape Analyser (Krüss) for each reagent and dosage were performed.

Prior to the start of contact angle measurements, the centimetre-sized block samples of the minerals were polished and the exposed surface was carefully cleaned through immersion in aqua regia (HNO_3 1:3 HCl, in a molar ratio) solution. Thereafter, the sample was subjected to ultrasound emissions for five minutes and intensively washed with ethanol and distilled water. Therefore, this cleaned polished mineral plate was conditioned for five minutes with the depressant, one minute with the etheramine collector, and ten minutes with the amidoamine collector. The conditioning times followed were the ones recommended by the reagent supplier, since they raise the concern that the new amidoamine collector provided was less soluble than etheramine. Consequently, a longer conditioning time was followed to ensure the adsorption efficacy. It is important to mention that even though the recommendations from the provider were followed, it was not observed any differences in the contact angle measurements when applying a conditioning time of one and ten minutes.

The pH was adjusted with sodium hydroxide or hydrochloric acid, when necessary. The contact angle measurements were performed in triplicate for each reagent, dosage, and pH analysed, and the average values were calculated.

These measurements were performed using only etheramine (dosage of 50, 75, 100, and 200 mg/L), only amidoamine (dosage of 50, 75, 100, and 200 mg/L), etheramine with starch (75 mg/L of collector and 215 mg/L starch), and amidoamine with starch (75 mg/L of collector and 215 mg/L starch). A reference measurement with only water was also performed. All the tests were performed at 3 different pH levels: 8, 10, and 11.

2.5. Zeta potential

Zeta potentials of hematite, quartz, and kaolinite were obtained through electrophoretic mobility measurements using a Zetasizer Nano (ZS90) system (Malvern Panalytical). The tested reagents were etheramine, amidoamine, and corn starch. NaOH and HCl were used as pH modifiers. The pure minerals were comminuted below 37 μm and the size was then reduced below 5 μm in an agate mortar. A small amount of the mineral powder was then conditioned with the reagent at a fixed concentration in a beaker and an aliquot of the supernatant solution with the mineral particles was analysed under the following conditions:

- Without reagents
- With etheramine (75 mg/L)
- With amidoamine (75 mg/L)
- With etheramine (75 mg/L) + starch (0.25 mg/L)
- With amidoamine (75 mg/L) + starch (0.25 mg/L)

Evaluations under each of the above conditions were conducted at pH 8, 10, and 11. All zeta potential tests were performed three times for representative purposes.

2.6. Flotation

The flotation efficiency of three collectors (etheramine, oleate, and amidoamine) was evaluated through kinetic flotation tests, performed with pure mineral samples of hematite, quartz, and kaolinite and the mixture of these minerals. The reagents used are listed in Table 1. Each flotation test was performed with 30 g of mineral sample (pure or mixed) in 15% solids content in a Minimet self-aerated flotation machine with a 400 mL cell. All flotations tests were performed three times for representative purposes.

Table 3
Test parameters for the flotation studies.

Reagents	Conditioning time (min)	Dosage (g/t)	pH
Etheramine	5	300	10
Oleate	5	300	Hematite, Quartz: 10 Kaolinite: 7.5 and 10
Amidoamine	5	300	10
Starch	5	1000	10

The flotation tests using a single mineral system were performed to better understand the specific interactions of the tested reagents with a specific mineral. In the first stage of testing, pure samples of quartz, hematite and kaolinite were floated at pH 10 and using 50, 100, 200, 300 and 400 g/t of amidoamine to determine the best dosage to perform flotation with this collector. After assessing the best dosage, the pH was varied to 11, 10, 9, 8 and 6.5 to assess the effect of pH on the collector's performance.

In the second stage of testing, pure samples of quartz were floated at pH 10 using etheramine, amidoamine, and etheramine with starch. Pure samples of kaolinite were floated using etheramine, amidoamine, etheramine with starch at pH 10, oleate at pH 7.5, and oleate at pH 10. Pure samples of hematite were floated using etheramine, amidoamine, etheramine with starch, and oleate at pH 10. The tests with the mineral mixtures (hematite-quartz; hematite- kaolinite) were performed at pH 10.

After performing the tests with pure mineral systems, the single-mineral flotation system was changed to a two-mineral system to understand the specific impacts that the presence of quartz and kaolinite could have on the flotation of hematite. The mass distributions in terms of hematite minerals and quartz were set with the objective of replicating the mass ratios of some itabirite ores from the Iron Quadrangle. Consequently, a distribution comprising 85% hematite and 15% quartz was selected to study the separation efficiency between quartz and hematite. Additionally, a mineral mixture composed of 85% hematite and 15% kaolinite was used for the two-mineral flotation system.

For the tests using etheramine, amidoamine , oleate, and starch, a conditioning time of 5 min was used. Flotation was performed at pH 10 with dosages of 300 g/t (this dosage was determined by the studies that will be shown later) for the three collector reagents and 1000 g/t for starch. However, for the tests with oleate, additional tests were conducted at pH 7.5 when studying the impacts of hematite with kaolinite.

The test parameters are described in Table 3.

2.7. Infrared measurements

Infrared spectroscopy was performed to study the adsorption of the amidoamine collector on to the surface of minerals such as hematite, quartz and kaolinite. Two types of samples were prepared for IR analysis:

- pure minerals, which were treated with water
- minerals treated with a collector solution at different collector concentrations at pH 10

Infrared (IR) spectra were measured using a laboratory Fourier transform infrared spectrometer (BRUKER IFS 55), equipped with a large-band mercury cadmium telluride (MCT) detector cooled at 77 K. Before the analysis, 2 g of pure minerals (hematite, quartz and kaolinite) with a granularity of 20–40 μm was conditioned. The conditioning lasted 60 min and was performed in a 50 mL solution of distilled water, 25 °C and collector at pH 10 (adjusted to pH 10 by addition of NaOH). The total concentration of amidoamine collector was varied from 10^{-4} to 5.10^{-3} Mol per litre. After agitation, the slurry was filtered and the liquid phase was rejected. Then, the solid phase of minerals samples was washed five times with 50 mL of deionized water at pH 10, filtered and dried in a desiccator. When dried, samples were sent immediately for analysis. Sample preparation for this analysis involved mixing 50 mg of sample with 280 mg of potassium bromide (KBr). All the diffuse reflectance (DRIFT) spectra are recorded with a 2 cm-1 spectral resolution. Each sample was scanned 200 times, duration of the analysis was 90 s. The influence of atmospheric water was subtracted.

3. Results and discussions

3.1. Contact angle measurements

Fig. 4 shows the contact angles, on the quartz surface, obtained at pH 8, 10 and 11 using etheramine (a) and amidoamine (b) at 0, 50, 75, 100, 200 mg/L collector dosage. The contact angles measured in the presence of etheramine on the quartz surface were greater than those obtained with amidoamine at all pH values tested.

Although smaller than the contact angles for etheramine, the angles obtained with amidoamine at pH 8 and 10 showed that this collector could hydrophobicise the quartz surface to promote its flotation, considering the analysed dosages.

The adsorption of the collectors on the mineral surface is dependent on pH, therefore the values of the contact angle depend on the collector's pK_a. The molecular structure of the collector is also an important factor affecting the contact angle. The favorable arrangement of adsorbent species due to the collector-collector interactions, for example, can generate different angular distributions of the collector in the adsorption layer. Considering different collectors, with different molecular structures, different contact angles with the same pH are expected.

The results presented in the Fig. 3 and Fig. 4 allow to deduce a higher surface -hydrophobization with ethermaine compared to amidoamine for all concentrations tested. The contact angle values depend on the collector concentration. On contact with water, the minerals showed a contact angle of approximately 10°. This angle increases with the introduction of the collector, towards angles that range from 31° to 72°. For both amidoamine and etheramine there was a tendency that higher dosages caused a subsequent drop in the contact angle. It was possible to observe that the optimal collector dosages were about 75 mg/L for etheramine and between 50 and 75 mg/L for amidoamine. This optimum range varies depending on the reagent structure and pH. In this case, a possible reason for the decreases in the contact angles at high collector dosages was due to the formation of a collector double layer on the mineral surface and/or micelle formation.

At pH 11, the lowest contact angles are observed for both collectors. Regarding the etheramine and its interaction with quartz at pH 11, the contact angle reduction was due to the increase in the RNH_2 molecules, which decreased the adsorption of the collector owing to the low electrostatic forces.

Fig. 5 presents the contact angles obtained as the result of the interactions between hematite and etheramine with and without starch (a), and the interactions between hematite and amidoamine with and without starch (b). It was observed that when using etheramine without a depressant, the contact angle obtained was between 34 and 36° (pH 8 and 10), i.e. a hydrophobicity level allowing the flotation of hematite. The contact angle decreased to 13° at pH 11 showing that this pH should promote the least flotation of hematite in comparison with pH 8 and 10. However, when considering the results obtained in Fig. 4, which showed that the contact angle measured for both etheramine and amidoamine on quartz was also the lowest at pH 11, it can be concluded that pH 11 was not optimal to promote the selective separation between hematite and quartz. On the other hand, the contact angle on the hematite sample with amidoamine changed negligibly, remaining below 20°.

The contact angles measured for the hematite conditioned in 215

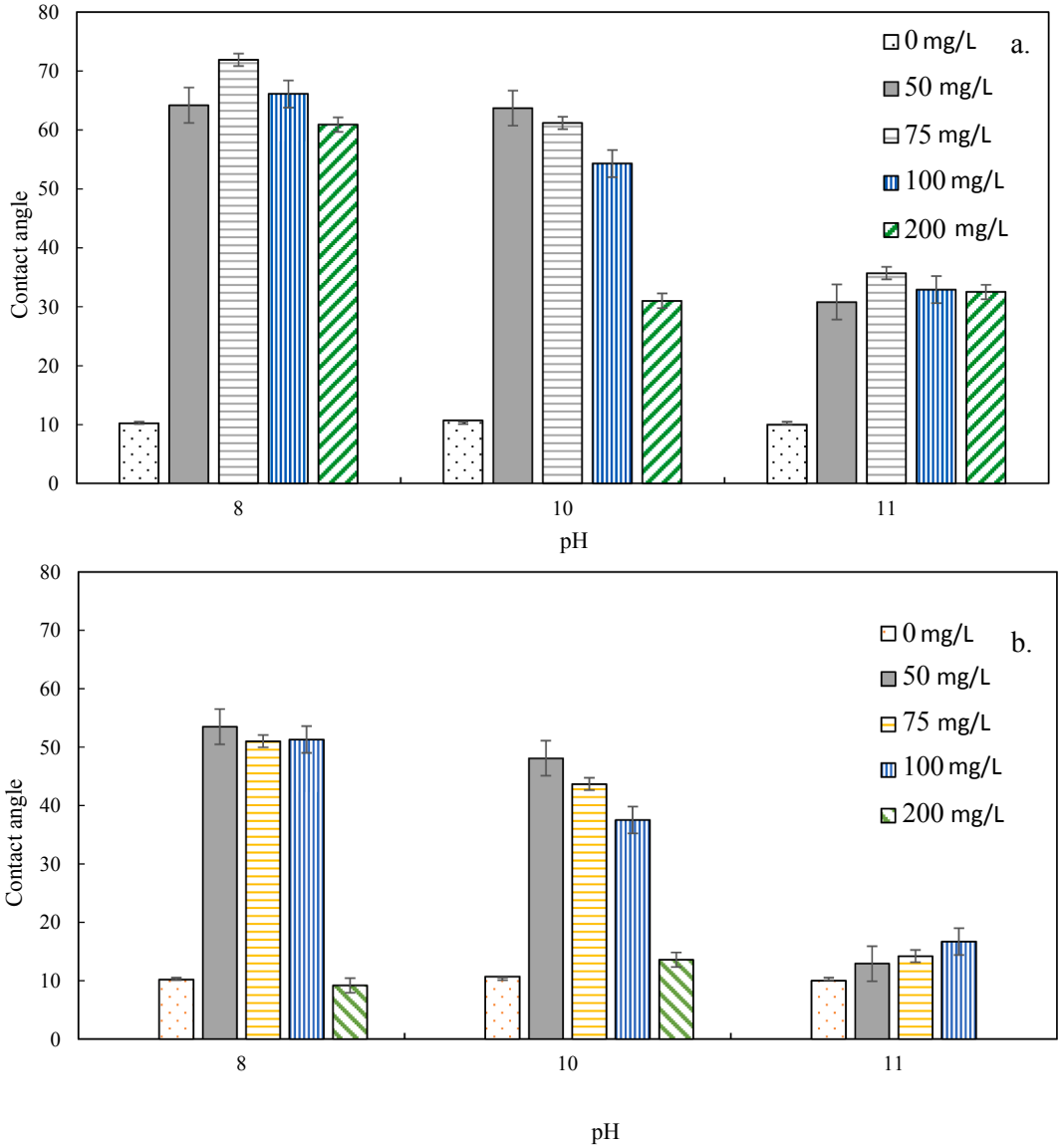

Fig. 4. Contact angle measurements on quartz mineral with standard deviation (SD) estimated based on three experiments. (a) Obtained using aqueous solutions of etheramine. (b) Obtained using aqueous solutions of amidoamine.

mg/L of starch solution were close to 10°, indicating efficient surface hydrophilisation, which is consistent with previously reported results regarding starch adsorption on hematite surfaces (Araujo et al., 2005; Kar et al., 2013; Severov et al., 2013). A considerable distinction was observed when comparing the contact angles measured in the presence of starch and etheramine versus the angles obtained in the presence of starch and amidoamine.

At pH 8 the contact angle measured using only etheramine dropped with the addition of starch (from 37 to 11°). On a smaller scale, the same decreasing effect was observed with amidoamine upon the addition of starch, with the contact angle dropping from 17 to 9°. At pH 10, in the presence of only etheramine the contact angle measured was about 34°, with the addition of starch the angle dropped to about 10°. At the same pH, the contact angle measured using solely amidoamine was about 12°, which with the addition of starch remained at about 12°. This shows that, for etheramine, the presence of starch is crucial to impeach the hydrophobization of the hematite surface. Contrary to what was observed for etheramine, the collector amidoamine showed a similar contact angle with and without starch, especially for pH 10 and 11. This similarity indicates that starch is not required to perform a selective flotation between quartz and hematite when using amidoamine at pH 10.

Fig. 6 presents the contact angle measurements on quartz at pH 8, 10 and 11 with etheramine (a) and amidoamine (b), considering a collector dosage of 75 mg/L, with and without starch. Regarding the etheramine collector results, the contact angle of quartz at pH 8 and 10 was reduced in the presence of starch but increased at pH 11, when compared to the angles at the same collector dosage (75 mg/L) without starch.

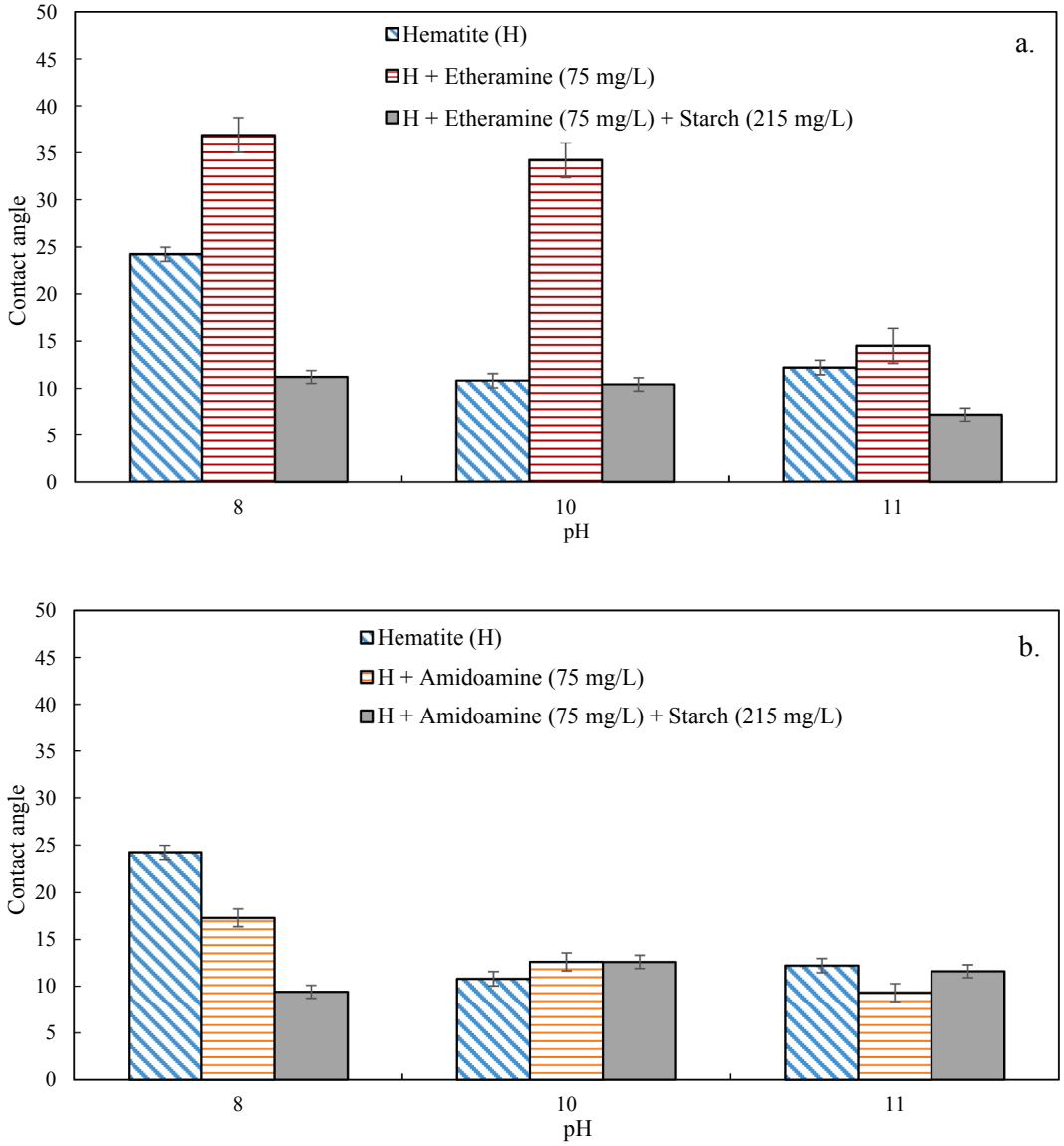

Fig. 5. Contact angle measurements on hematite with SD estimated based on three experiments. (a) Without reagents, in an aqueous solution of etheramine with and without starch. (b) Without reagents, in an aqueous solution of amidoamine with and without starch. Dosage: 215 mg/L of starch, 75 mg/L collector).

The interaction of quartz with amidoamine after conditioning with starch showed that the contact angles increased slightly at pH 10 compared to those with no starch at the same collector dosage but dropped significantly at pH 11, as observed in Fig. 6.

3.2. Zeta potential measurements

Surface coverage was assessed by comparing the zeta potential values upon varying pure starch dosages from zero to 500 mg/L and the resultant surface charge of hematite, quartz and kaolinite after reagent adsorption. Starch concentrations chosen for these tests were a low one, 0.25 mg/L, and a high dosage, 215 mg/L, for adsorption comparison. The concentrations of collectors used in these tests were 75 mg/L for adsorption comparison between the standard collector etheramine and the amidoamine. The zeta potential measurements of hematite, quartz and kaolinite obtained in the presence of starch with etheramine and starch with amidoamine are shown in Figs. 7 and 8 respectively.

Fig. 7 shows that the low and the high starch dosage associated with the collector etheramine (75 mg/L) resulted in close to zero surface charges for quartz and kaolinite at pH 10 (Fig. 7 a. and b.). Diversely, for hematite the low dosage with ethereamine was not sufficient to cover the hematite surface, leaving exposed negative surface charges (-15.3 mV) that were only neutralized by the higher starch dosage 215 mg/L, reversing the hematite surface charge to + 1.72 mV (Fig. 7c). By comparing Fig. 7 to Fig. 8 it can be observed that the surface charges resultant from the amidoamine adsorption onto quartz were more negative, meaning that higher dosages of this collector should be evaluated for denser surface coverage.

Similar to the contact angle studies on the quartz and hematite surface, the collector dosage selected to analyse the zeta potential was 75 mg/L. Both etheramine and amidoamine modified the surface charge of hematite, quartz, and kaolinite (Figs. 9, 10 and 11). The zeta potential values observed for hematite and quartz agreed with previously reported results obtained using pure water and in the presence of etheramine (Filippov et al., 2010; Veloso et al., 2018).

Increases of approximately 25 and 15 mV in the positive surface charge were observed for hematite in the presence of etheramine at pH 8 and 10, respectively, when compared to the reference (hematite without reagent) (Fig. 7a). These findings are consistent with the trends and values observed by Filippov et al. (2010). The zeta potential increased

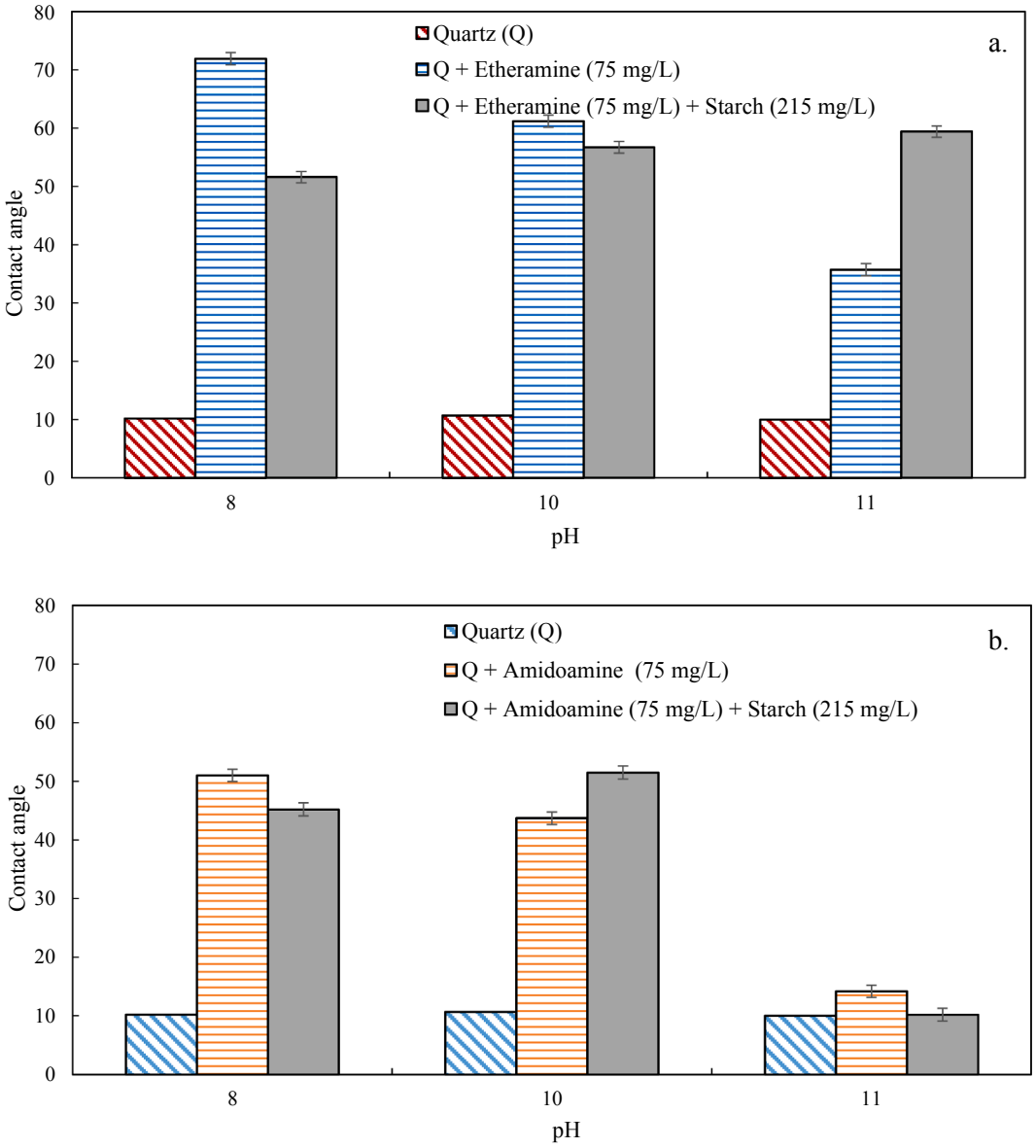

Fig. 6. Contact angles on quartz at pH 8, 10 and 11 in aqueous solutions of (a) etheramine and starch. (b) amidoamine and starch. Collector dosage: 75 mg/L. Starch dosage: 215 mg/L.

by approximately 55 mV when hematite was conditioned with amidoamine at pH 8.

The increase in the zeta potential at pH 8 and 10 in the presence of etheramine and amidoamine for quartz and kaolinite (Fig. 10 and Fig. 11) when compared to that of the reference (without reagent) can be explained by the negative charge compensation due to the adsorption of collectors through the amine groups. However, the zeta potential increased significantly at pH 8 for amidoamine, whereas the zeta potential variation for etheramine was slightly pronounced at pH 10. The values of the zeta potentials were similar for both the collectors at pH 11. This shows that the biggest difference in the adsorption behaviour between both collectors occurs at pH 8 and 10, a similar result that was already observed and discussed based on the contact angle studies in section 3.1. The proximal values of the zeta potentials for the amine at pH 11 in all the tested minerals can be explained by the pK values close to 10.5, observed for the amine collectors (Smith and Scott, 1990). The decreased concentration of the ionic forms of the collectors decreases their adsorption on the mineral surface at an alkaline pH higher than 10.5.

The surface charge values of hematite and kaolinite in the presence of starch and etheramine are slightly higher than those obtained only using etheramine. These results confirm the different adsorption behaviours of starch on kaolinite and quartz. They corroborate the findings of Ma and Bruckard (2010), explaining that the adsorption behaviour of starch on the quartz surface cannot be extrapolated to that on kaolinite in reverse cationic flotation of iron ores. The adsorption of starch on the hematite surface is controlled by hydrogen bonding and chemical complexation (Weissenborn et al., 1995). The adsorption density of starch on the quartz surface is lower than that on the hematite surface and is controlled by hydrogen bonding (Filippov et al., 2013). Thus, depending on the hydrolysis of the surface groups, the adsorption of starch may lead to additional surface charge compensation.

Another hypothesis for this phenomenon observed in quartz with etheramine and starch could be the formation of clathrates(Aguiar et al.,

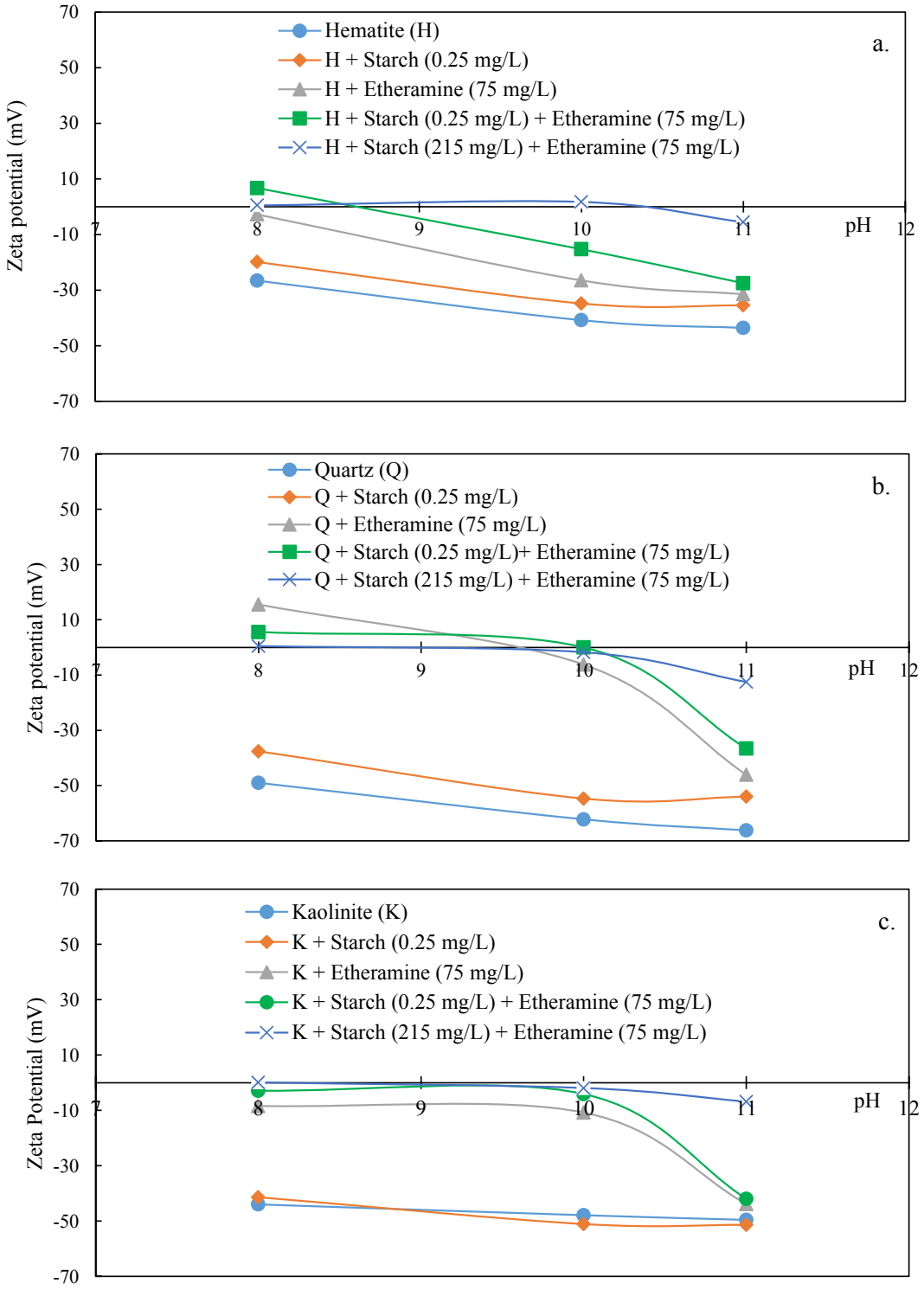

Fig. 7. Zeta potential of hematite (a), quartz (b) and kaolinite (c) with starch and etheramine.

2017) . The complexes between starch and etheramine can lead to higher adsorption of etheramine on the quartz surface, contributing to the reduction in the zeta potential. However, the intermolecular hydrogen bonding between the amylose chains and hydroxyl groups of the glucose molecules in starch leading to helicoid formation and then to starch–amine clathrate aggregates is observed only at higher starch concentrations. According to Khosla and Biswas (1984), free starch molecules are adsorbed at the active sites of the mineral surface until saturation is reached. In this case, starch adsorption resulting in clathrate formation will not follow the linear pattern observed in the experimental data provided by Filippov and co-workers (Filippov et al., 2013). Thus, another explanation for this phenomenon is that starch can co-absorb at the quartz–solution interface, in association with etheramine.

The presence of starch did not considerably change the zeta potential of any of the minerals with amidoamine. The results presented in this section in combination with the contact angle measurements suggest that amidoamine is a potential collector for iron ore beneficiation,

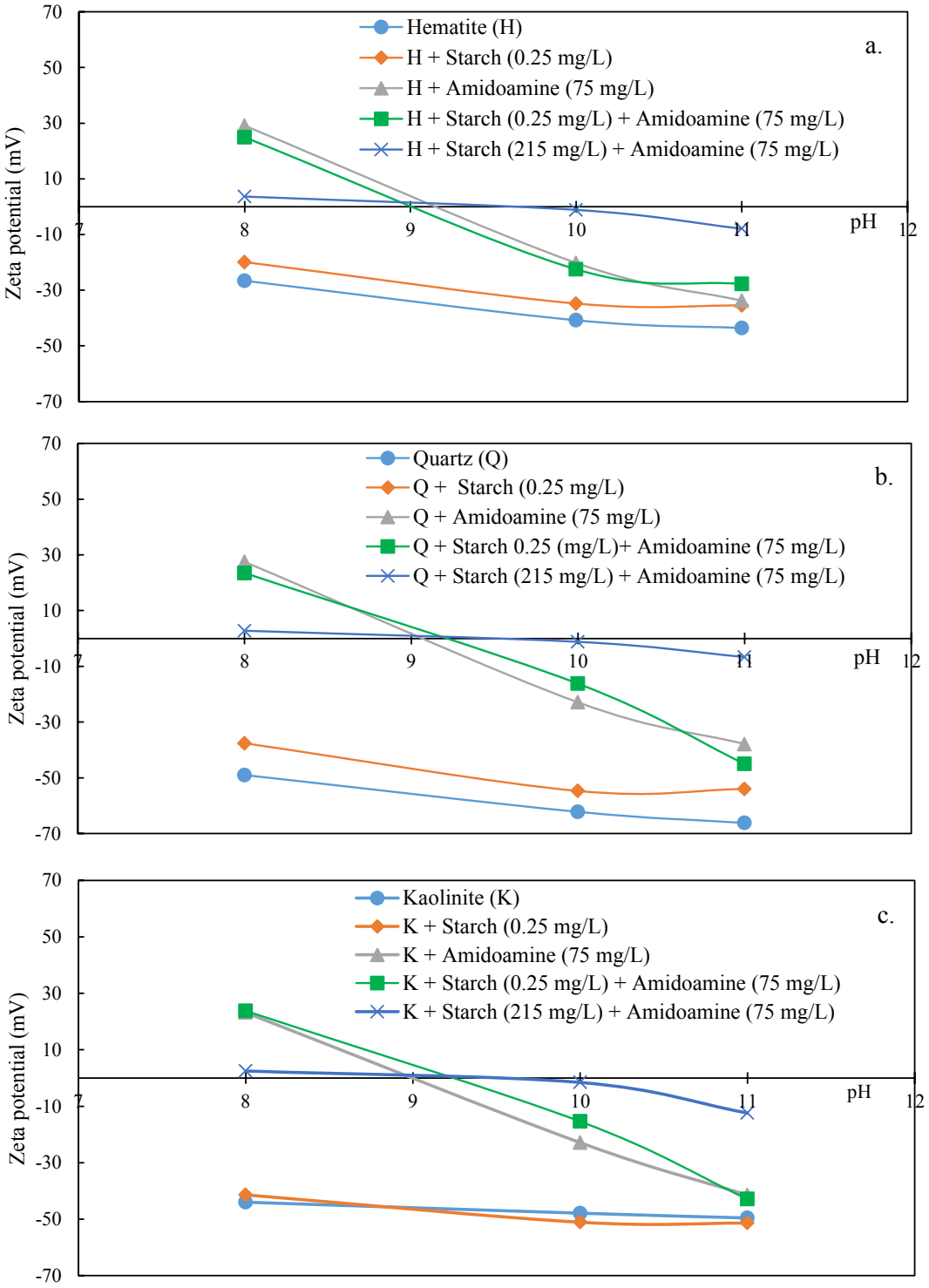

Fig. 8. Zeta potential of hematite (a), quartz (b) and kaolinite (c) with starch and amidoamine.

specifically because it can promote the selective flotation of quartz and hematite without a depressant. The following section presents the findings of the flotation experiments performed with the pure minerals and mineral mixtures.

3.3. Flotation of pure minerals

Table 4 shows the results of the flotation tests with a single mineral system: hematite, quartz and kaolinite at pH 10 at 50, 100, 200, 300 and 400 g/t of amidoamine.

The results showed that at the dosages of 50 and 100 g/t no hematite was recovered to the floated product. Hematite started to report to the floated product at 200 g/t (1% recovery), with the maximum hematite recovery (12% recovery) achieved when dosing 400 g/t. Contrarily to hematite, quartz reported to floated product at 50, 100 and 200 g/t, achieving 18, 43 and 70% recovery respectively. Kaolinite started to report to the floated product at 300 g/t, achieving 10% recovery at 400 g/t.

Based on the results presented in Table 4 and discussed above, the dosage of 300 g/t was selected to perform the future flotation studies. This dosage was selected since at 300 g/t the hematite recovery to

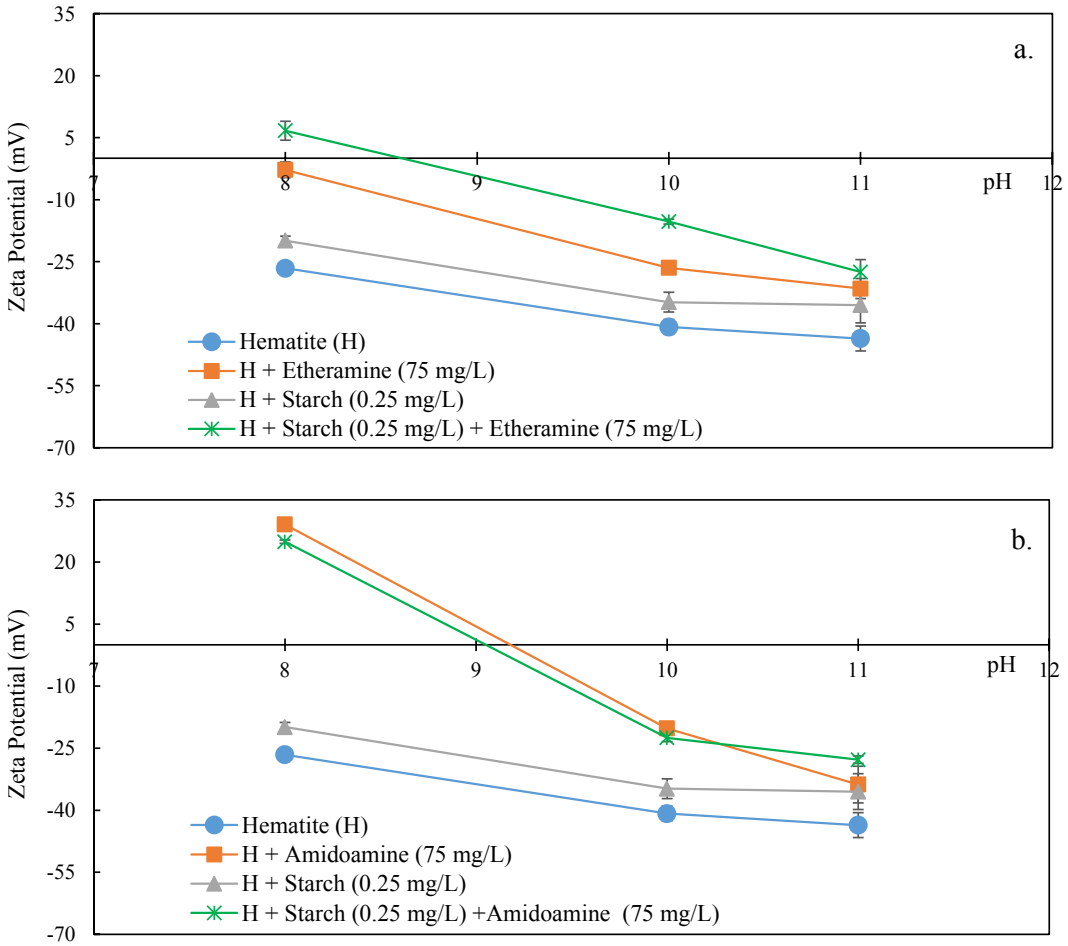

Fig. 9. Zeta potentials of hematite under different experimental conditions (SD is shown on the graph and the value varies between 0.6 and 4.4). (a) Hematite with etheramine. (b) Hematite with amidoamine.

floated product was still considerably close to 0% (app. 1% recovery) while the recovery of quartz was at 89%. In the other words, this dosage could promote a selective flotation of quartz while providing lower losses of hematite to the floated product. Table 5 shows the results of the flotation tests with a single mineral system: hematite, quartz and kaolinite at 300 g/t of amidoamine at pH 6.5, 8, 9, 10 and 11 (see Table 6 and Table 7).

The results show that the recovery of quartz was higher at more low pH values. The recovery of quartz was the lowest at pH 11 (44%), increasing to 89% at pH 10, to 94% at pH 9 and to 100% at pH 8. Hematite recovery to floated increased by about 8% when the pH value decreased from 10 to 9. Hematite reported a relatively constant recovery to the floated product (10 to 13%) at pH 9, 8 and 6.5. Kaolinite recovery was the highest at pH 6.5, with 6% recovery.

The decrease in the flotation response of the quartz at pH11 is in perfect agreement with the contact angle measurements and can be related related to pKa ≈ 8.2 value (communicated by Clariant) when the molecular forms of collectors dominate in the solution with less adsorption capacity on the negatively charged mineral surface.

Based on the results summarized in table 5, the value of pH 10 was adopted to continue the future flotation studies because it was the pH value that reported the lowest loss of hematite to the floated product (app 1% recovery) while providing a recovery of quartz of 89%.

3.3.1. Hematite

The flotation kinetics curves for hematite obtained using the etheramine, etheramine with starch (reverse cationic flotation), amidoamine and oleate at pH 10 are presented in Fig. 12.

Both oleate and etheramine (without starch) promoted hematite flotation (Fig. 12). Oleate enabled greater mass recovery in the floated product for the same specific dosage at 300 g/t. The pure hematite flotation tests performed with amidoamine as the collector showed that no hematite was floated. This absence of hematite flotation is in accordance with the contact angle measurements for hematite with amidoamine. Moreover, when comparing the hematite recovery to the floated fraction by etheramine (68%) versus the recovery obtained with etheramine and starch (0%) it becomes visible that the presence of starch was essential to inhibit the flotation of hematite by etheramine, contrary to amidoamine which did not required the addition of starch to inhibit hematite flotation.

3.3.2. Kaolinite

The flotation kinetics curves for pure kaolinite obtained using the etheramine, etheramine with starch (reverse cationic flotation), amidoamine and oleate at pH 10 are presented in Fig. 13.

The etheramine floated 51% of kaolinite, a result that remained relatively unchanged upon the addition of starch. The floatability obtained when using etheramine can be explained by the high specific surface area of the kaolinite, which may require higher doses of the collector. Some studies have reported that kaolinite has characteristics that pose challenges during concentration through cationic collectors, such as amines. The kaolinite crystal system has an anisotropy that causes it to behave in a manner opposite to that of quartz in terms of the pH dependence on cationic flotation (Xu et al., 2015). The flotation of

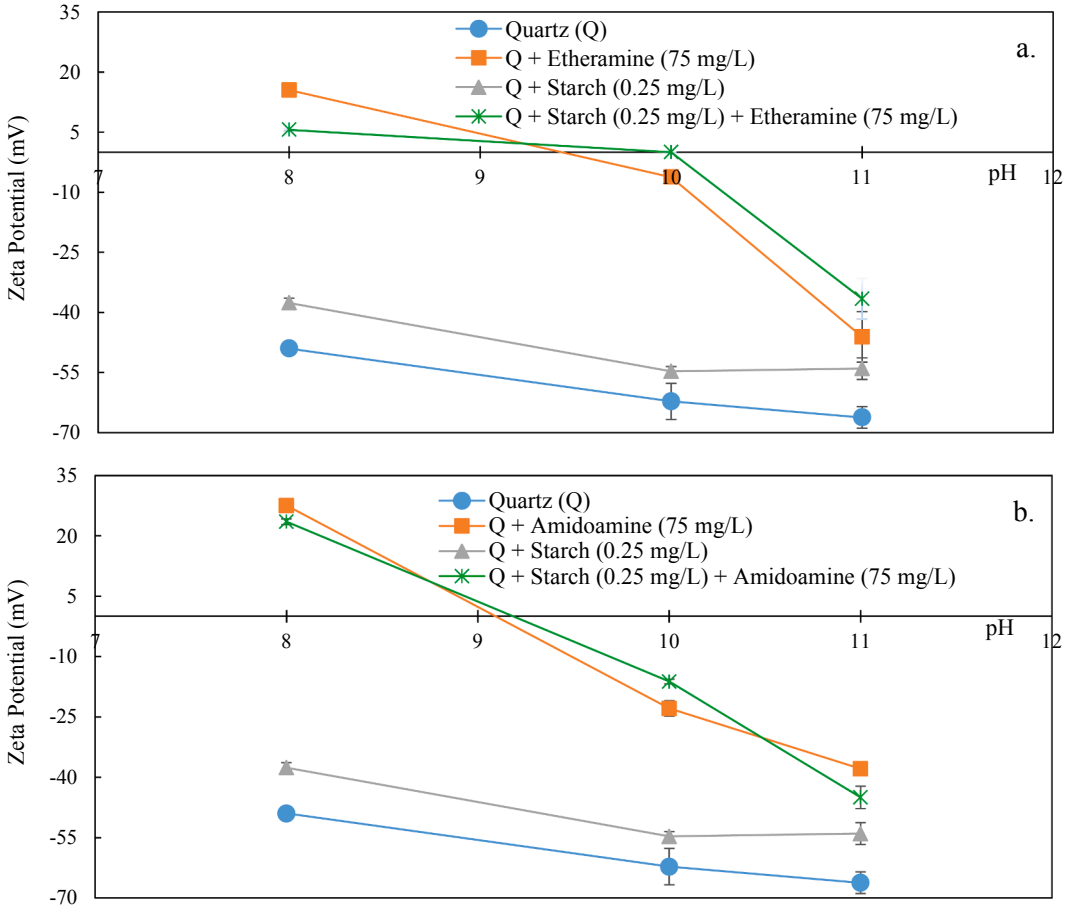

Fig. 10. Zeta potentials for quartz under different experimental conditions (SD is shown on the graph and the value varies between 0.3 and 6.3). (a) Quartz with etheramine. (b) Quartz with amidoamine.

the fine kaolinite particles is also impacted by the increased number of edges to adsorb the amines in a cationic form which decreases adsorption layer density.

When varying the pH to obtain more alkaline values, the negative surface charges of the oxides and silicates are enhanced, thereby increasing the adsorption of the cationic collector and, consequently, the floatability of the mineral. Ma et al., (2009) reported that the flotation behaviour of quartz cannot be extrapolated to that of kaolinite owing to the face-edge structure of kaolinite. Kaolinite is an aluminosilicate that has two different surfaces parallel to the (001) plane in its structure: a (001) plane formed from the tetrahedral sheet (SiO_4) and the second plane formed from the AlO_6 octahedron (Liu et al., 2015). At an alkaline pH, preferential adsorption occurs at the SiO_4 basal plane. Hydrophobic aggregation seems to occur owing to the chain–chain associations between collector molecules adsorbed at the SiO_4 basal plane. Consequently, the (001) planes of AlO_6 are exposed, thus reducing the floatability of kaolinite (Xu et al., 2015). The basal (001) plane exhibits a strong affinity for cationic collectors and is responsible for kaolinite flotation, whereas the AlO_6 plane has limited interactions with cationic collectors and remains hydrophillic (Yuehua et al., 2004). Thus, preliminary conditioning with starch does not impact kaolinite flotation because of two competing phenomena: hydrogen bonding between the hydroxyl groups of starch and alumina tetrahedron and repulsion between anionic starch molecules and negatively charged basal planes of the silanol surface (Ma and Bruckard, 2010).

Oleate did not promote the flotation of pure kaolinite at pH 10. At pH 7.5, it could enable flotation of approximately 20% of the kaolinite at a dosage of 300 g/t. Owing to the anisotropic structure of kaolinite, the zeta potential on the surface of each plane varies differently in relation to the pH. The isoelectric point of the AlO_6 face is between pH 6 and 8 and the same for the SiO_4 face is observed at approximately pH 4 (Gupta and Miller, 2010). As oleate is an anionic collector, physical adsorption seems to occur at pH 7.5 because the surface charge of the AlO_6 face in kaolinite is positive. However, the mass recovery is low (23%) at a dosage of 300 g/t. At pH 10, no flotation occurred owing to physical adsorption because of the high hydroxyl ion concentration. Thus, the amidoamine at dosage of 300 g/t did not promote a significant kaolinite recovery to the floated product.

3.3.3. *Quartz*

The flotation kinetics curves for pure quartz obtained using each reagent are presented in Fig. 14.

The quartz recovery obtained when only using amine is considerably similar to the recovery obtained when using amine with starch, meaning that starch had virtually no depression effect on quartz flotation. Literature suggests that a lack of quartz depression does not mean that there is no adsorption of starch to the surface of quartz (Filippov et al., 2013). Several authors reported starch adsorption on hematite and not on quartz surface (Balajee and Iwasaki, 1969; Cooke et al., 1952; Peres and Correa, 1996). Pavlovic and Brandão (2003) showed a decrease in the floatability of quartz in the presence of starch while the flotation of hematite flotation was depressed. Moreover, the adsorption studies performed with different polysaccharides led to conclude about the starch adsorption on the hematite, quartz and other silicates (Pavlovic

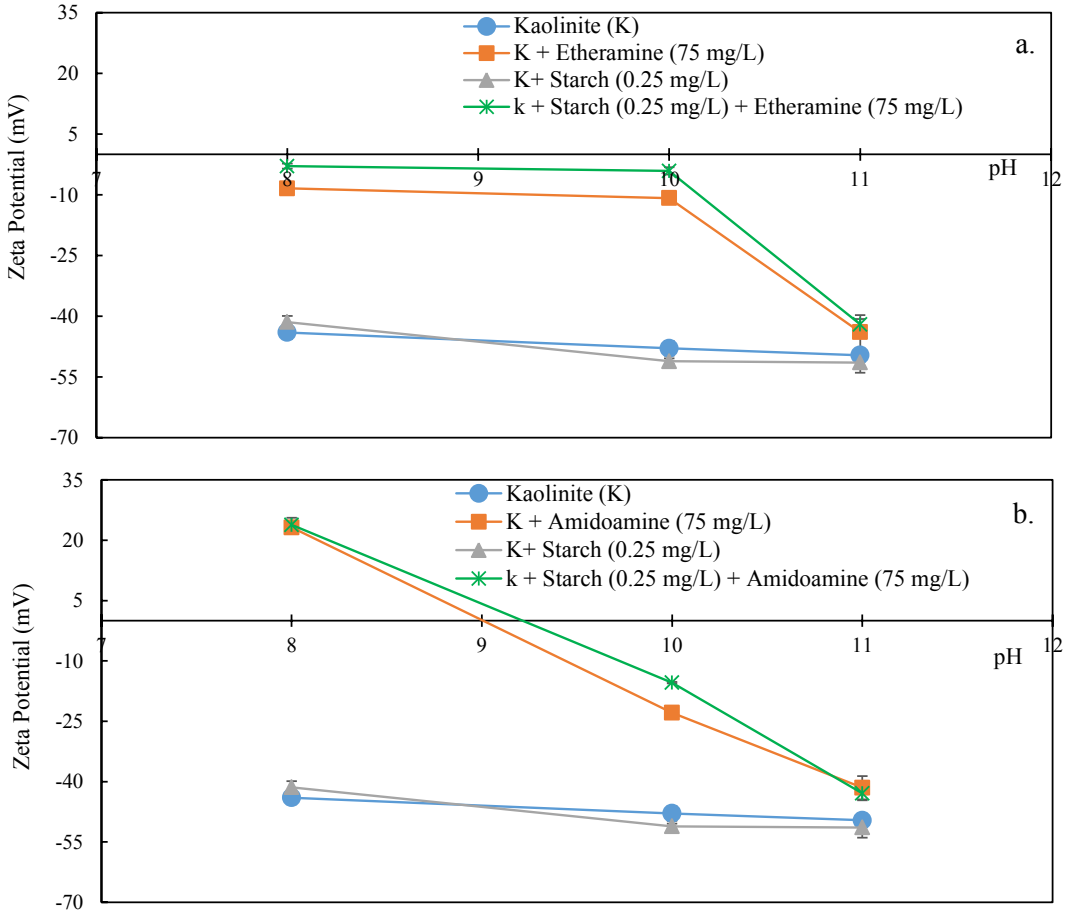

Fig. 11. Zeta potential for kaolinite under different experimental conditions (SD is shown on the graph and the value varies between 0.6 and 2.9): (a) Kaolinite with etheramine. (b) Kaolinite with amidoamine.

Table 4
Recovery of hematite, quartz and kaolinite (single mineral flotation system) to the floated fraction at pH 10 at 50, 100, 200, 300 and 400 g/t of amidoamine.

Amidoamine dosage (g/t)	Recovery to floated (%)		
	Hematite	Quartz	Kaolinite
50	0	18	0
100	0	43	0
200	1	70	0
300	1	89	1
400	12	97	10

Table 5
Recovery to the froth product of hematite, quartz and kaolinite at 300 g/t of amidoamine as a function of pH (single mineral flotation system).

pH	Recovery to floated (%)		
	Hematite	Quartz	Kaolinite
11	1	44	3
10	2	89	1
9	10	94	3
8	11	100	1
6.5	13	98	6

and Brandão, 2003; Dogu and Arol, 2004, Filippov et al., 2013). However, the starch adsorption on the quartz was difficult to confirm using the surface sensitive techniques, i.e. infrared spectroscopy. Pavlovic and Brandão (2003) suggested that the very intense IR absorption bands of quartz in the same wavenumber area where important carbohydrates bands occur makes the detection of the polysaccharides difficult. Severov et al. (2013) and Filippov et al. (2013) agreed that hydrogen bonding is difficult to confirm from the IR spectra because starch molecules are capable of forming intramolecular hydrogen bonds. However, analyzing the vibration band of the other involved groups (C-O stretch and C1/H deformation) they have proved the hydrogen bonding on the quartz from the FTIR spectra.

The amidoamine collector promoted quartz flotation. However, for the same collector dosage of 300 g/t, etheramine achieved a higher mass recovery. The mass recovery when only using etheramine was almost 100% after 6 min of flotation versus 88% recovery with amidoamine.

3.4. Flotation of mineral mixtures

3.4.1. Mixture: 85% hematite and 15% quartz

The flotation kinetics curves for the hematite–quartz mixture are presented in Fig. 15.

The results presented in Fig. 15 agree with those available in the literature (Araujo et al., 2005) indicating that a depressant is necessary for quartz during direct flotation of hematite with oleate to obtain adequate selectivity in the concentration process. For recovering approximately 100% of the hematite in the froth product with oleate, a recovery of approximately 45% was achieved for quartz as well.

Similarly, a depressant was found to be required for hematite during quartz flotation using amine collectors to achieve adequate selectivity in the concentration process. When using only etheramine almost 100% of the quartz and 50% of hematite reported to the froth product. The hematite recovery to the floated fraction by etheramine dropped to 3% upon the addition of starch.

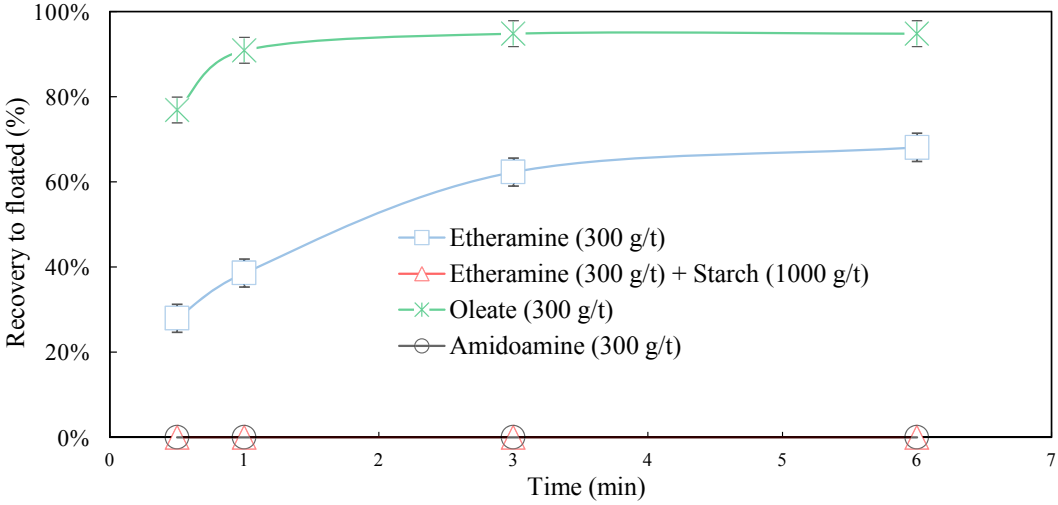

Fig. 12. Hematite recovery in bench-scale tests using etheramine, etheramine with starch, oleate and amidoamine at pH 10.

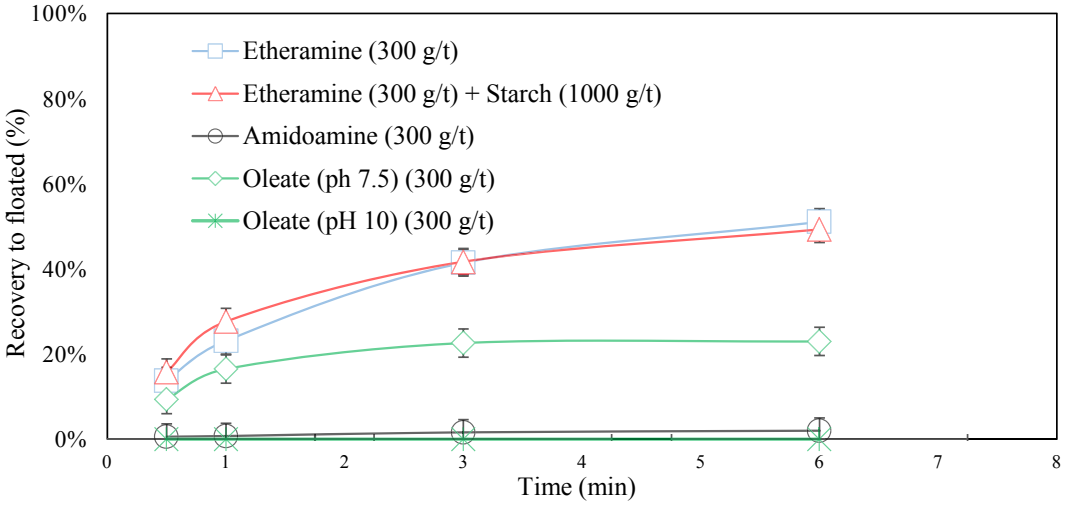

Fig. 13. Kaolinite recovery in bench-scale tests at pH 10 with etheramine, etheramine with starch, amidoamine and oleate (pH 7.5 and 10).

The reverse flotation of quartz using amidoamine reported satisfactory results without the addition of starch. This collector enabled 100% recovery of quartz to the floated fraction, whereas approximately 94% of the hematite was not floated. One of the possible reasons for the rejection of approximately 6% iron content when using amidoamine in the flotation process may be due to hematite dragging in the froth during the flotation of quartz (entrainment and entrapment).

A considerable selectivity was attained by using amidoamine as collector without any depressant. The starch has an unselective flocculation effect of particles under 5 μm (Weissenborn et al., 1995). In conventional operations of iron ore beneficiation by flotation, the flotation feed is deslimed to remove the 10 μm fraction prior to flotation (Filippov et al 2014), thus the unselective flocculation effect of starch does not affect the flotation selectivity. Contrary to what occurred in this study, where the pure mineral samples used for the flotation tests were not deslimed. Therefore, it could be stated that by using amidoamine, additionally to eliminating the necessity of a depressor agent in the reverse flotation of iron ore may as well eliminate the necessity of having a desliming stage before the flotation process.

Fig. 16 shows that higher specific dosages (g/t SiO_2) of amidoamine improved the recovery of quartz, reaching 100%. The results of the flotation tests conducted for a mixture of pure minerals indicate that is possible to obtain selective flotation of quartz in the reverse approach without a depressant. However, to reach the same recovery level as that achieved using the amine collector, it is necessary to use a higher dosage of amidoamine than etheramine.

3.4.2. Mixture: 85% hematite and 15% kaolinite

The flotation kinetics curves for the hematite–kaolinite mixture are presented in Fig. 17.

Regarding the direct flotation of hematite with oleate, at pH 10, approximately 95% hematite and (Fig. 17a) 16% kaolinite were recovered (Fig. 17b). The oleate collector showed good selectivity, indicating the possibility of direct flotation (considering the hematite / kaolinite composition) without using depressants.

In the reverse flotation of kaolinite with etheramine without a depressant, 57% of the kaolinite mass was floated (Fig. 17b), whereas approximately 7% of hematite mass was floated (Fig. 17a). The use of starch reduced kaolinite recovery to 43% to the floated fraction (Fig. 17b), maintaining the hematite recovery at 7% (Fig. 17a).

The results obtained for the flotation of pure hematite and hematite–kaolinite mixture using the etheramine collector are shown in Fig. 18.

The recovery of iron oxide reduced from 68% to approximately 7% in the presence of 15% kaolinite. The presence of kaolinite appears to inhibit the cationic flotation of hematite by the etheramine. As

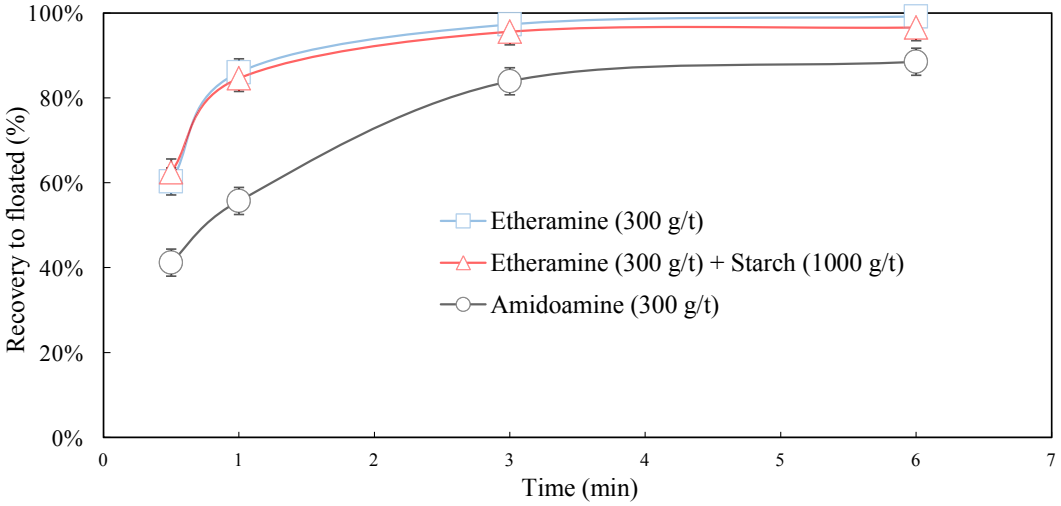

Fig. 14. Quartz recovery in bench-scale tests with etheramine, etheramine plus starch, and amidoamine.

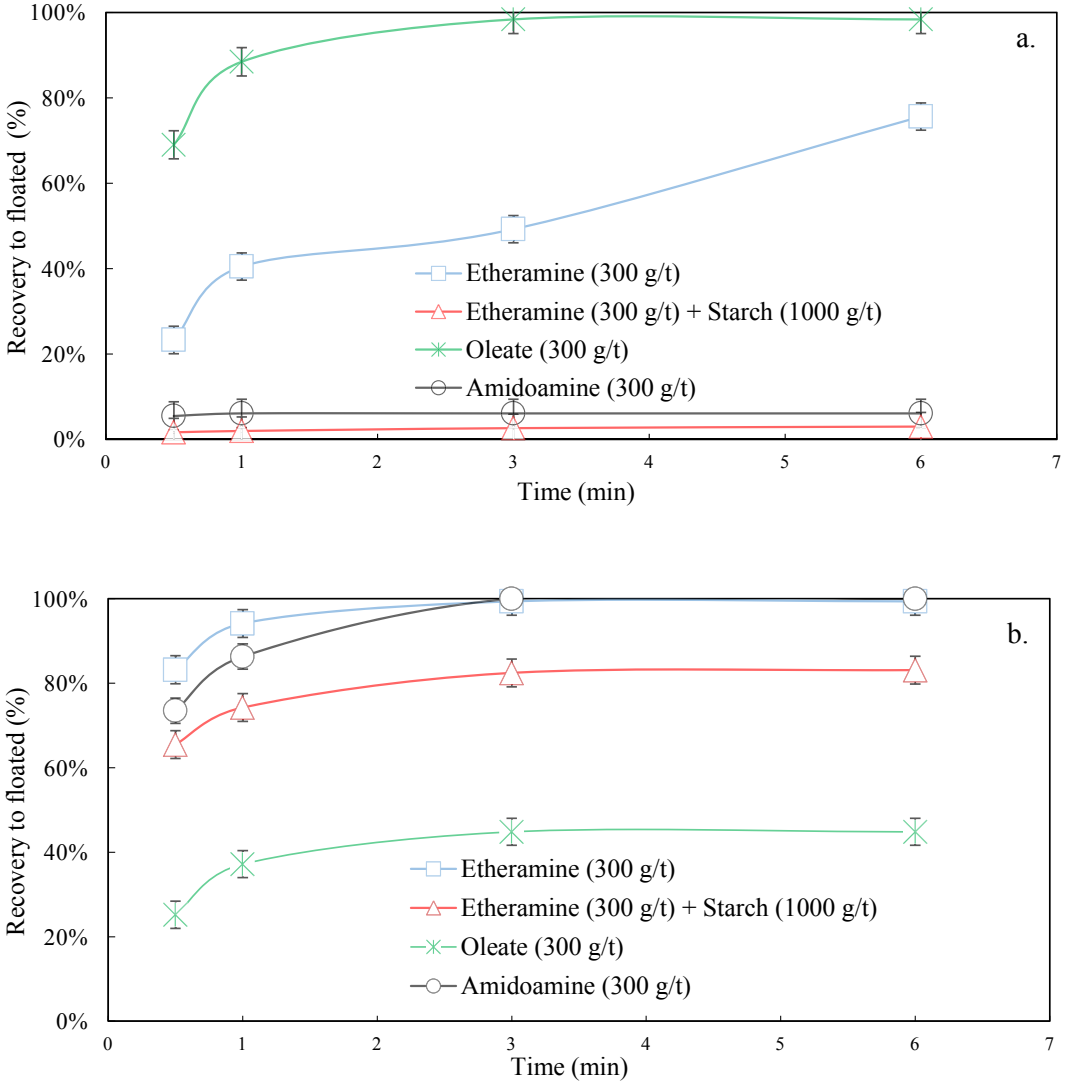

Fig. 15. Flotation test results of the hematite–quartz mixture at pH 10: (a) Hematite recovery. (b) Quartz recovery.

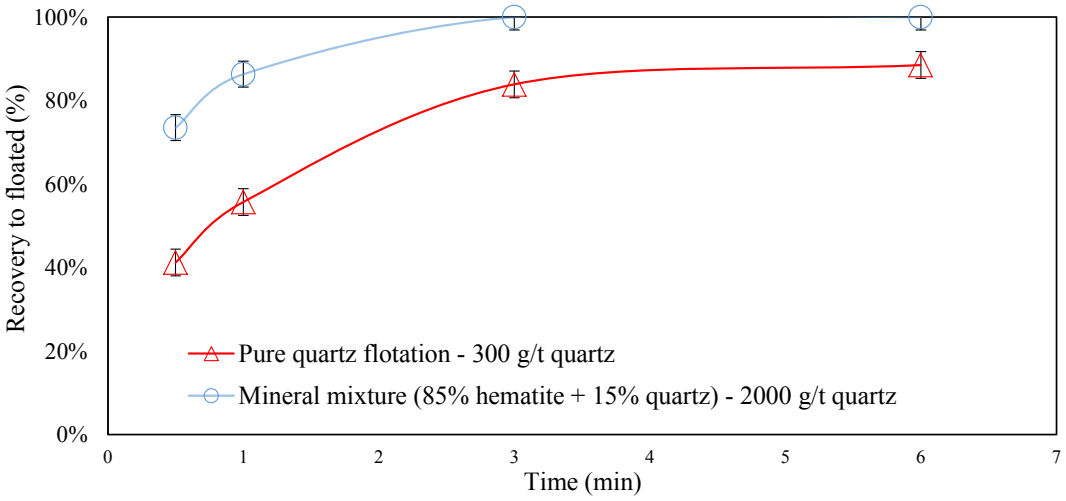

Fig. 16. Quartz recovery using amidoamine on pure quartz sample and in hematite–quartz mixture at pH 10.

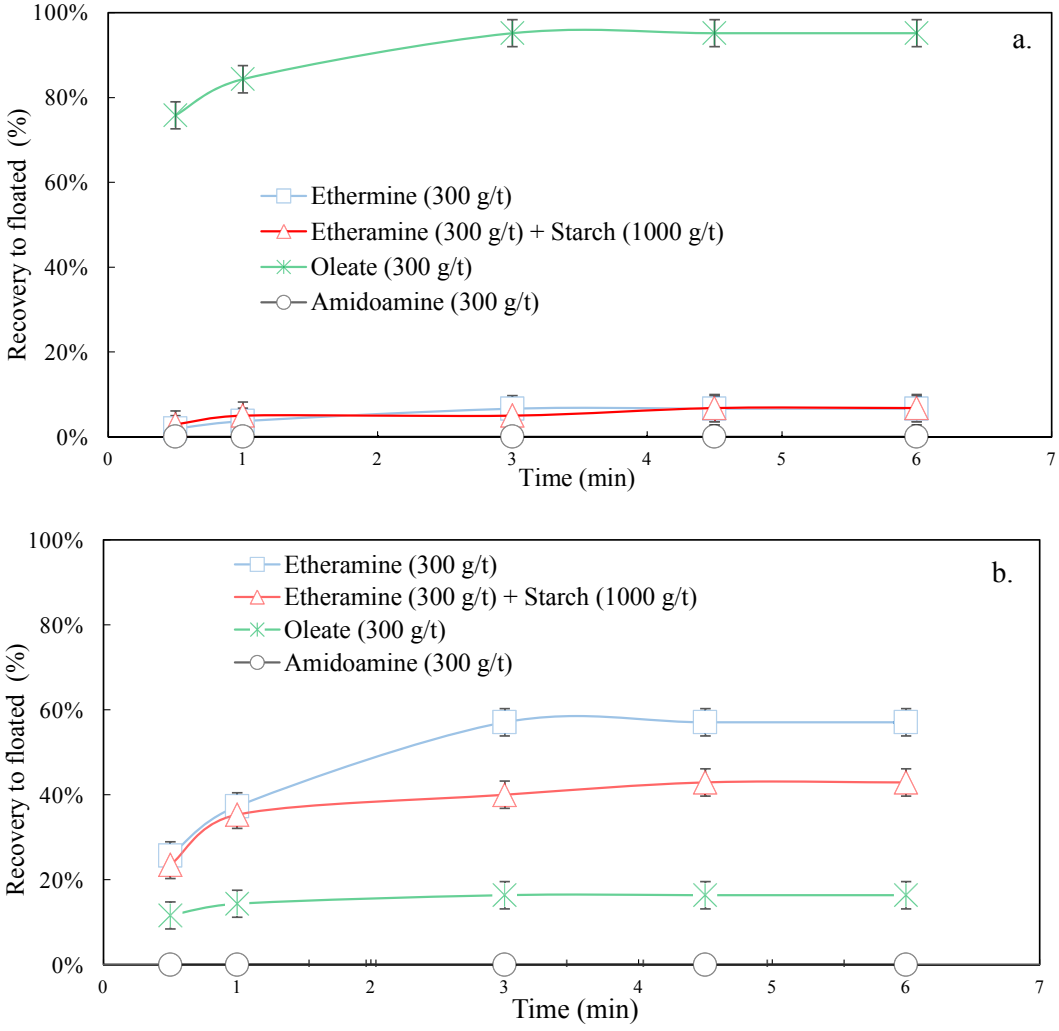

Fig. 17. Flotation recovery results of the hematite–kaolinite mixture at pH 10: (a) Hematite recovery. (b) Kaolinite recovery.

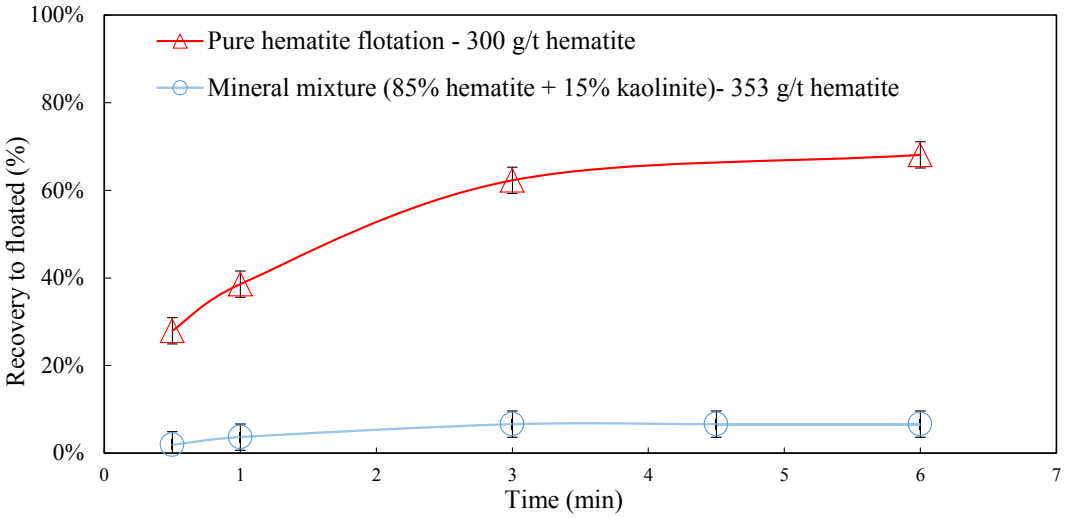

Fig. 18. Hematite recovery during flotation tests of pure hematite and hematite–kaolinite mixture using etheramine collector at pH 10.

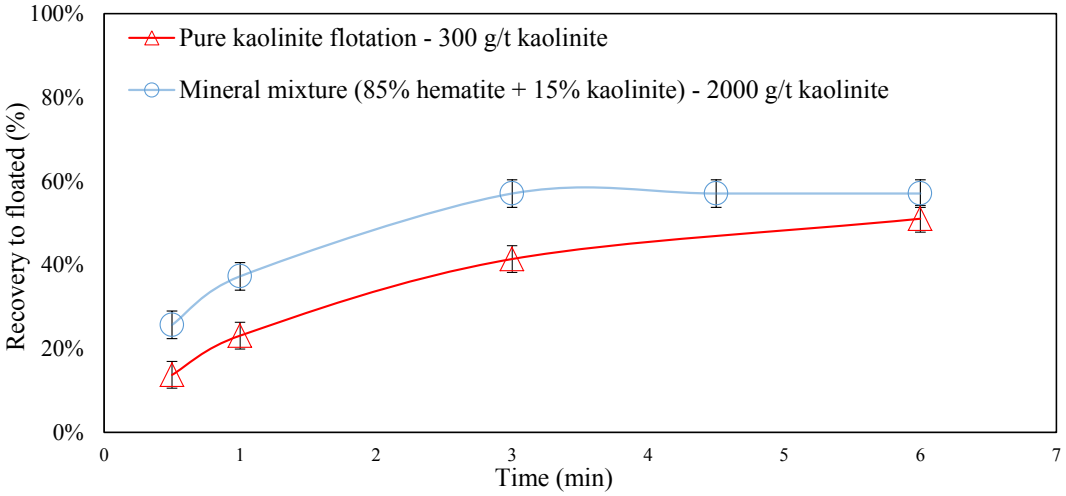

Fig. 19. Kaolinite recovery in the flotation tests using kaolinite and hematite–kaolinite mixture using etheramine collector.

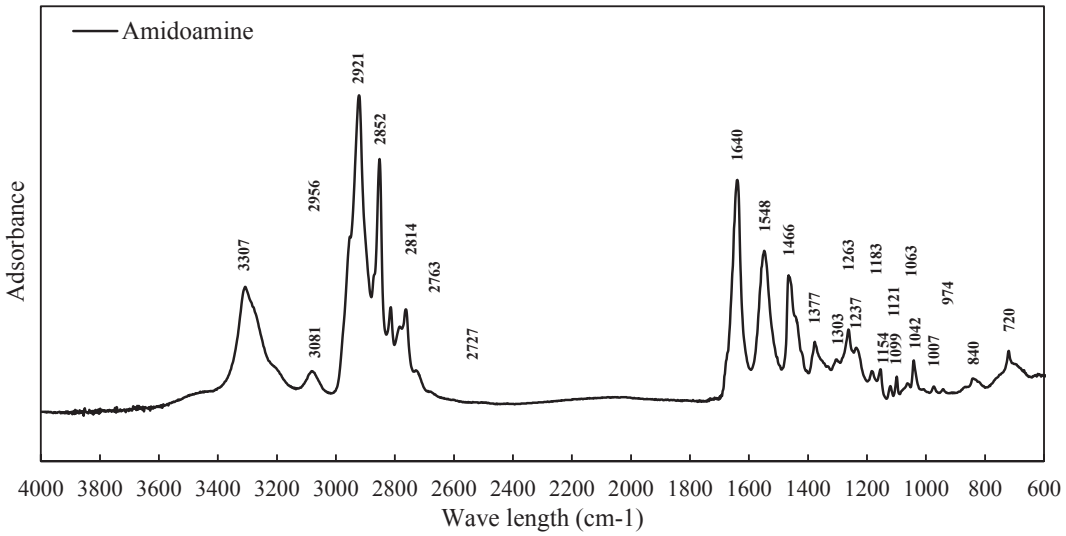

Fig. 20. The FTIR spectra obtained for the amidoamine collector.

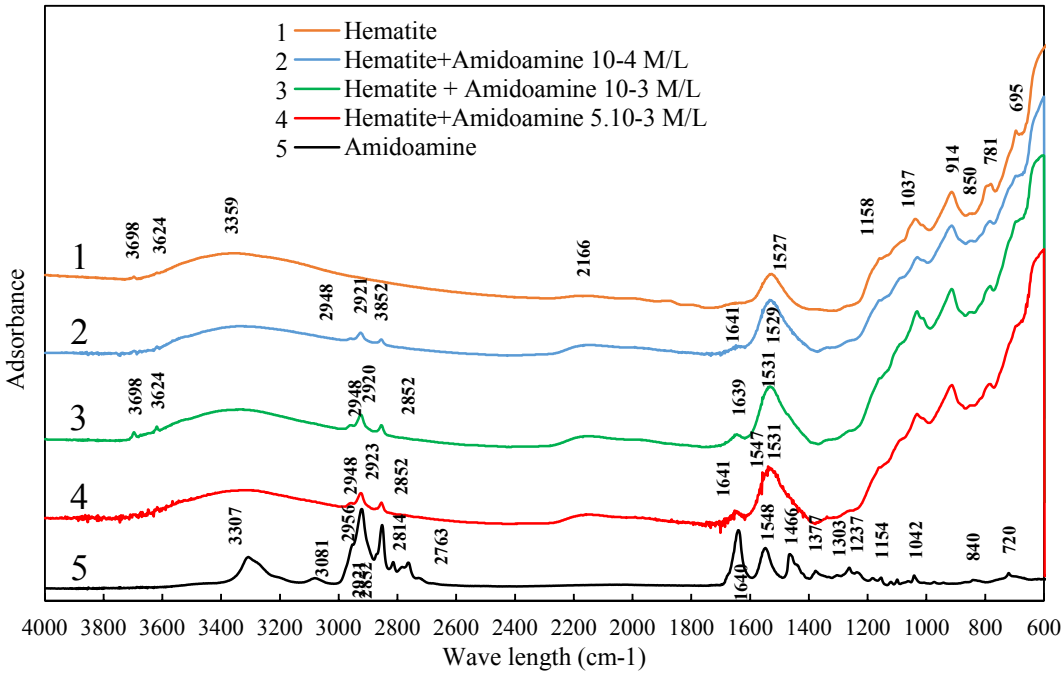

Fig. 21. FTIR spectra of hematite before (1) and after interaction with amidoamine (2, 3, and 4).

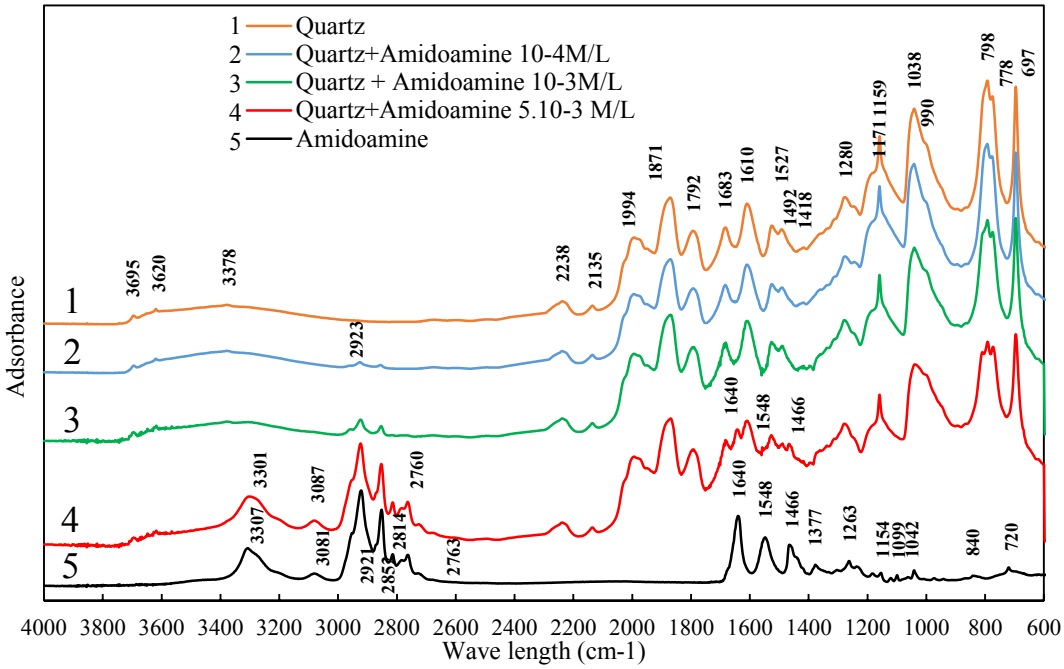

Fig. 22. FTIR spectra of quartz before (1) and after interaction with amidoamine (2, 3, and 4).

mentioned previously, the SiO_4 face on kaolinite is capable of adsorbing etheramine, but the flotation of kaolinite is hampered by an anisotropy in its structure.

When compared to pure kaolinite flotation, the kaolinite recovery after 6 min of flotation showed an increase from 51% (pure kaolinite flotation) to 57% (kaolinite flotation in the hematite–kaolinite mixture), as shown in Fig. 19. However, although the total collector dosage was the same in both tests, the specific dosage of the collector (g/t kaolinite) varied from 300 g/t (pure kaolinite sample) to 2000 g/t (hematite–kaolinite mixture).

For the results obtained using amidoamine with the hematite–kaolinite mixture, the same results as those obtained in the pure mineral flotation tests were obtained; that is, the amidoamine collector did not float kaolinite and hematite at a dosage of 300 g/t.

3.5. Infrared measurements

Three types of samples were analyzed: 1) pure amidoamine, 2) pure minerals (hematite, quartz and kaolinite), and 3) minerals after the addition of amidoamine. Fig. 20 shows the FTIR spectra obtained for amidoamine. The FTIR spectra obtained for hematite, quartz, and kaolinite, before and after the interaction with three distinct dosages of

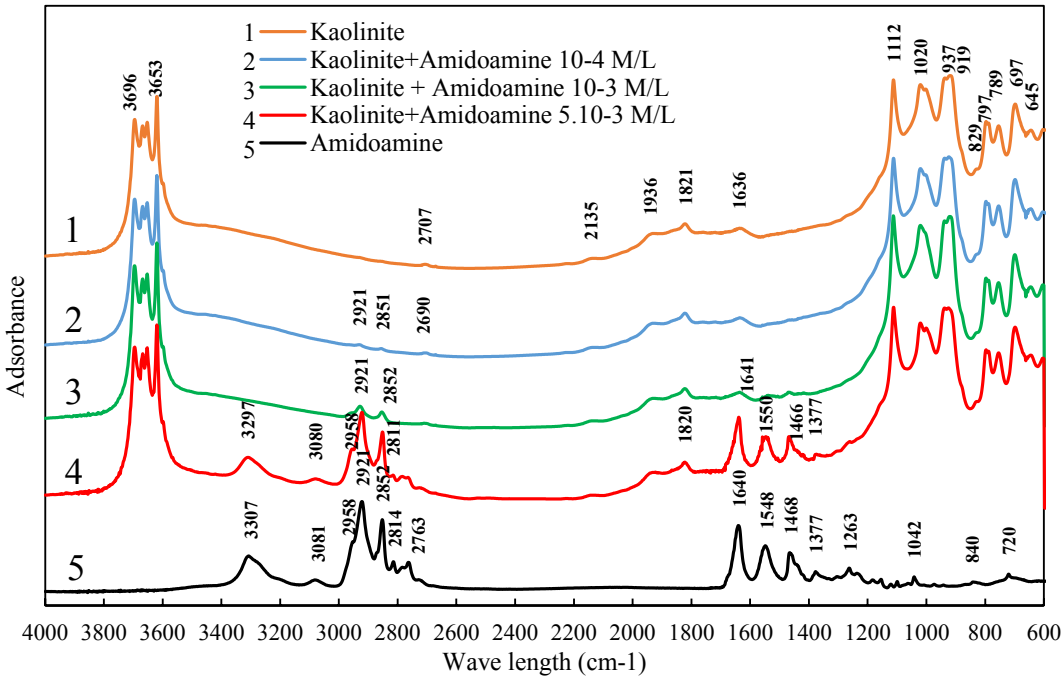

Fig. 23. FTIR spectra of kaolinite before (1) and after interaction with amidoamine (2, 3, and 4).

Table 6
Peaks and corresponding groups in the 2 800 and 3300 cm–1 domain.

ID	FTIR data (cm^{-1})				
Symmetry		Symmetric stretching of (CH_2)	Asymmetric stretching of (CH_2)	Asymmetric stretching of (CH_3)	Symmetric stretching of (CH)
Group	(ν(NH))	($\nu_s(CH_2)$)	($\nu_{as}(CH_2)$)	($\nu_{as}(CH_3)$)	($\nu_s(CH_2)$)
Wave number (cm^{-1})	3307	2852	2921	2 956	2814

Table 7
Identification of the presence of a collector on the surface of minerals.

Mineral	Concentration (M /L)	Wave number (cm-1)							
		ν(NH)	νs(CH2)	νas(CH2)	νas(CH3)	νs(CH2)	C = O	NH	CH3 + scissoring of CH2
Amidoamine	Pure	3307	2852	2921	2 956	2814			
Quartz	10–4		2852	2923					
	10–3		2852	2923					
	5.10^{-3}		2852	2923	2956	2814	1640	1548	1466
Kaolinite	10–4		2852	2921					
	10–3		2852	2921					
	5.10^{-3}		2852	2923	2956	2811	1641	1550	1466
Hematite	10–4		2852	2921					
	10–3		2852	2921					
	5.10^{-3}		2852	2923					

the amidoamine collector are presented in Figs. 21, 22 and 23 respectively.

The characteristics bands (cm^{-1}) identified for the amidoamine collector (Fig. 20) were: 3307, 3081, 2921, 2852, 2814, 2763, 1640, 1548, 1466, 1377, 1263, 1042, 840, 720.

The spectra obtained for the amidoamine collector showed two main domains of absorbance (Fig. 20). The first domain is located between 2700 and 3300 cm^{-1} (Tables 6 and 7), characteristic of the C-H and NH bond vibrations. The four peaks at 2852 cm^{-1}, 2921 cm^{-1}, 2956 cm^{-1}, 2814 cm^{-1} respectively correspond to the asymmetric elongation vibrations of the group ($\nu_s(CH_2)$), ($\nu_{as}(CH_2)$), ($\nu_{as}(CH_3)$) in the hydrocarbon chain and the symmetric stretching ($\nu_s(CH)$) of carbon bound to nitrogen (C-H)-N. The peaks at 3307 and 3081 cm^{-1} corresponds to the stretching and harmonic vibration of NH of amidoamine collector respectively.

The second domain is located between 1640 and 600 cm^{-1}. In this region, the FTIR spectra showed a strong absorption band at 1640 cm^{-1}, which is characteristic of C = O amide. The peak 1548 correspond to the angular deformation of NH while the peak at 1466 cm^{-1} to asymmetric bending of CH_3 + scissoring (in-plane symmetric bending) of CH_2 and 1377 cm^{-1} - symmetric bending of CH_3.

After interaction with amidoamine, new bands at around 2921 and 2852 cm^{-1} for kaolinite, around 2923 and 2852 cm^{-1} for quartz and 2923 and 2852 cm^{-1} for hematite were assigned to the stretching bands of $–CH_3$ and $–CH_2$ groups in amidoamine when the concentration of the collector increases (Table 7). The bending and stretching vibration of N–C bonds of amidoamine appeared at 1466 cm^{-1} for kaolinite and 1466 cm^{-1} for quartz, respectively.

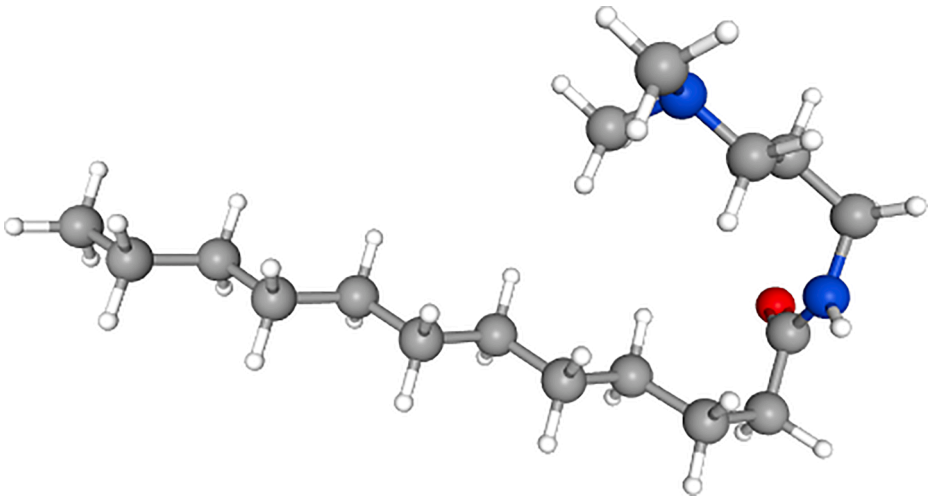

Fig. 24. Chemical structure of N-[3-(Dimethylamino)propyl]dodecanamide (Copied from PubChem, 2020).

The conventional amines used in the reverse flotation of iron ore (e.g., etheramine) are cationic collectors, meaning that when in water they adopt a positive charge and adsorb to negatively charged silicate gangue minerals by electrostatic forces to promote their flotation (Filippov et al., 2014, Nakhaei and Irannajad, 2017).

Contrary to etheramine, the amidoamine showed a selective flotation of quartz in mineral samples composed of hematite and quartz without the need for a depressant at the pH values where both two mineral surfaces display negative charges. Fig. 24 shows the amidoamine N-[3-(Dimethylamino)propyl]dodecanamide chemical structure.

The amidoamine N-[3-(Dimethylamino)propyl]dodecanamide molecule structure has a bond between the methyl and amine groups in the hydrophilic head of this reagent, which significantly increases the volume of the polar head in comparison with those of more conventional cationic collectors such as etheramine and makes this molecule more susceptible to steric hindrance effects (Fig. 24).

As mentioned by Chen et al., (2017), surfactants initially adsorb on mineral surfaces through electrostatic interaction as individual ions; further, with the increase in the coverage of the surfactant on the mineral surface, steric hindrance gradually occurs. Liu et al., (2019) used surface tension measurements, molecular dynamics simulations and density functional theory to investigate the effects of introducing an isopropanol substituent in amine collectors. The results showed that introducing this isopropanol substituent in dodecyl amine weakened the electrical properties of the polar groups and increased the cross-sectional size of these groups. Similar effects were demonstrated and reported previously by Filippov and co-workers when an aliphatic iso-alcohol reagent was used in combination with anionic collectors for calcium minerals flotation (Filippov et al., 2006; Filippova et al., 2014; Filippov et al., 2019) and with cationic collectors for reverse iron ore and silicates flotation (Filippov et al., 2010; Filippov et al., 2012, Filippov, 2017). The results obtained in our work are in agreement with the effect demonstrated by Liu et al. on the reverse flotation of quartz and hematite in relation to the performance of a collector with high steric hindrance (Liu et al., 2020). The results reported show that the increase in the steric hindrance improves the selectivity in relation to the cationic reverse flotation of these minerals.

The infrared spectra presented in Figs. 21 to 23 showed no difference in the adsorption behaviour of the amidoamine collector at a low concentration of 10^{-4} M/L, what is consistent with the zeta potential measurements (Fig. 8).

The intensity of peaks related to the stretching bands of CH_3 and CH_2 is the same or slightly higher on the hematite than in quartz and kaolinite. However, the peaks intensity increases significantly on the quartz and kaolinite for the concentration of 5.10^{-3} M/L of the collector (Figs. 22 and 23), pointing to a higher quantity of adsorption of the collector on silicate minerals, such does not occour for hematite (Fig. 21). This difference in adsorption behaviour is responsible for the selective flotation of quartz from hematite.

For quartz and kaolinite, the more intense peaks may be explained by the specific adsorption on the more negatively charged silicate minerals surface defined by the silica tetrahedron.

Since for this amidoamine collector the structure of the adsorption layer is controlled by the collector concentration, there is a hindrance effect for hematite. Such hindrance effects can be caused by characteristic as for example, molecular arrangements or interactions promoted by hydrogen bonding and/or electrostatic forces.

An increase in collector concentration leads to the increased quartz recovery due to the increased quantity of the collector deduced from the higher peak intensity (Fig. 16), while the flotation of hematite does not occur or is very low (Fig. 15a). However, the flotation behaviour of kaolinite is similar to those of hematite while the CH3 and CH2 peaks intensity is similar to the spectrum of quartz. The high specific surface area coupled with double sheet structure may be an explanation for this behaviour (Ma and Bruckard, 2010; Xu et al., 2015).

4. Conclusions

Contact angle measurements showed no significant hydrophobisation of the hematite surface with N-[3-(Dimethylamino)propyl] dodecanamide, despite the zeta potential studies showed a certain level of adsorption of this amidoamine on the hematite surface. The flotation studies corroborated with the interpretation made from the contact angle measurements by showing a low floatability for hematite and kaolinite while a total flotation of the quratz was observed.

The infrared spectroscopy results showed that an increase in amidoamine concentration did no result in a significant variation in peak intensity (stretching bands of CH_3 and CH_2) for hematite while the peaks intensity on the quartz and kaolinite were increased significantly.

The most adequate hypothesis for the mechanism responsible for the selective flotation of quartz with N-[3-(Dimethylamino)propyl] dodecanamide (without starch) is a hindrance effect due to the intermolecular interactions controlled by the collector concentration.

The new amidoamine collector was able to promote a selective flotation of quartz from hematite without a depressant agent, such as starch. Therefore, this reagent can be an advantageous alternative to conventional amines, currently used in reverse cationic flotation of iron ores.

Understanding the adsorption mechanism of this specific amidoamine may contribute to the development of a new class of collecting

reagents, more effective for reverse iron ore flotation, reducing or eliminating the need for the depressant reagent, also contributing to a decrease of iron loss to tailings.

CRediT authorship contribution statement

Klaydison Silva: Conceptualization, Resources, Investigation, Data curation, Validation, Writing - original draft, Writing - review & editing. **Lev O. Filippov:** Conceptualization, Resources, Validation, Supervision, Funding acquisition, Project administration, Writing - original draft, Writing - review & editing. **Alexandre Piçarra:** Investigation, Data curation, Validation, Writing - original draft, Writing - review & editing. **Inna V. Flilippova:** Data curation, Validation. **Neymayer Lima:** Methodology, Investigation. **Anna Skliar:** Investigation. **Lívia Faustino:** Methodology, Investigation, Data curation. **Laurindo Leal Filho:** Conceptualization, Resources, Methodology.

Declaration of Competing Interest

The authors declare that they have no known competing financial interests or personal relationships that could have appeared to influence the work reported in this paper.

Acknowledgments

This paper was supported by VALE S.A in the context of developing new beneficiation routes for iron ore. The support of Clariant, Brazil as a partner in this project is deeply appreciated. The technical support from the Steval staff at GeoRessources, University of Lorraine, is greatly acknowledged.

References

Aguiar, M., Furtado, R., Peres, A, 2017. Seletividade na flotação catiônica reversa de minerio de ferro. Holos 24 (11), 126–135.

Araujo, A.C., Viana, P.R.M., Peres, A.E.C., 2005. Reagents in iron ores flotation. Miner. Eng 18 (2), 219–224. https://doi.org/10.1016/j.mineng.2004.08.02.

Balajee, S.R., Iwasaki, I., 1969. Adsorption mechanism of starches in flotation and flocculation of iron ores. Trans. AIME 244, 401–406.

Chen, P., Hu, Y., Gao, Z., Zhai, J., Fang, D., Yue, T., Zhang, C., Sun, W., 2017. Discovery of a novel cationic surfactant: tributyltetradecyl-phosphonium chloride for iron ore flotation: From prediction to experimental verification. Minerals. 7, 240. https://doi.org/10.3390/min7120240.

Cooke, S.R.B., Schultz, N.F., Lindroos, E.W., 1952. The effect of certain starches on quartz and hematite suspensions. Trans. AIME 193, 697–698.

Dogu, I., Arol, A.I., 2004. Separation of dark-colored minerals from feldspar by selective flocculation using starch. Powder Technol. 139, 258–263.

Dos Santos, I.D., Oliveira, J.F., 2007. Utilization of humic acid as a depressant for hematite in the reverse flotation of iron ore. Miner. Eng. 20, 1003–1007. https://doi.org/10.1016/j.mineng.2007.03.007.

Filippov L.O., Filippova I.V., 2006. Synergistic effects in mix collector systems for non sulfide mineral flotation. Proc. of XXIII Int. Min Proc. Congress, Istanbul, Turkey, 3-8 September 2006 (Eds. Onal G. et al) pp. 631-634.

Filippov, L., Filippova, I., Severov, V., 2010. The use of collectors mixture in the reverse cationic flotation of magnetite ore. The role of Fe-bearing silicates. Miner. Eng. 23, 91–98. https://doi.org/10.1016/j.mineng.2009.10.007.

Filippov, L., Duverger, A., Filippova, I., Kasaini, H., Thiry, J., 2012. Selective flotation of silicates and Ca-bearing minerals : the role of non-ionic reagent on cationic flotation. Minerals Engineering 36–38 (10), 314–323.

Filippov, L., Severov, V., Filippova, I., 2013. Mechanism of starch adsorption on Fe-Mg-Al-bearing amphiboles. Int. J. Miner. Process. 123, 120–128. https://doi.org/10.1016/j.minpro.2013.05.010.

Filippov, L., Severov, V., Filippova, I., 2014. An overview of the beneficiation of iron ores via reverse cationic flotation. Int. J. Miner. Process. 127, 62–69. https://doi.org/10.1016/j.minpro.2014.01.002.

Filippov, L.O., Filippova, I.V., Lafhaj, Z., Fornasiero, D., 2019. The role of a fatty alcohol in improving calcium minerals flotation with oleate. Colloids and Surfaces A: Physicochemical and Engineering Aspects 560, 410–417.

Filippova, I.V., Filippov, L.O., Duverger, A., Severov, V.V., 2014. Synergetic effect of a mixture of anionic and nonionic reagents: Ca mineral contrast separation by flotation at neutral pH. Minerals Engineering 66–68, 135–144.

Filippov L. O. Flotation process for recovering feldspar from a feldspar ore., 2017. US Patent 9,675,980.

Fornasiero, D., Filippov, L.O., 2017. Innovations in the flotation of fine and coarse particles. J. Phys. Conf. Ser. 879, 012002 https://doi.org/10.1088/1742-6596/879/1/012002.

Friedli, F.E., 1990. Amidoamine surfactants. In: Cationic Surfactants - Organic Chemistry (Surfactant Science Series; v34). Marcel Dekker Inc., New York, pp. 52–83.

Gupta, V., Miller, J., 2010. Surface force measurements at the basal planes of ordered kaolinite particles. J. Colloid. Interface Sci. 344 (2), 362–371. https://doi.org/10.1016/j.jcis.2010.01.012.

Kar, B., Sahoo, H., Rath, S.S., Das, B., 2013. Investigations on different starches as depressant for iron ore flotation. Miner. Eng. 49, 1–6. https://doi.org/10.1016/j.mineng.2013.05.004.

Khosla, N.K., Biswas, A.K., 1984. Mineral–collector–starch constituent interactions. Colloids Surf. 9 (3), 219–235.

Lima, N., Silva, K., Souza, T., Filippov, L., 2020. The Characteristics of Iron Ore Slimes and Their Influence on the Flotation Process. Minerals. 10, 675. https://doi.org/10.3390/min10080675.

Liu, W., Liu, W., Zhao, Q., Shen, Y., Wang, X., Wang, B., Peng, X., 2020. Design and flotation performance of a novel hydroxy polyamine surfactant based on hematite reverse flotation desilication system. Journal of Molecular Liquids 301, 1–9. https://doi.org/10.1016/j.molliq.2019.112428.

Liu, J., Wang, X., Lin, Ch.-L., Miller, J.D., 2015. Significance of particle aggregation in the reverse flotation of kaolinite from bauxite ore. Minerals Engineering 78, 58–65. https://doi.org/10.1016/j.mineng.2015.04.009.

Liu, W., Peng, X., Liu, W., Wang, X., Zhao, Q., Wang, B., 2019. Effect mechanism of the iso-propanol substituent on amine collectors in the flotation of quartz and magnesite. Powder Technol. 360, 1117–1125. https://doi.org/10.1016/j.powtec.2019.10.060.

Ma, X., Bruckard, W.J., 2010. The effect of pH and ionic strength on starch–kaolinite interactions. Int. J. Miner. Process. 94, 111–114. https://doi.org/10.1016/j.minpro.2010.01.004.

Nakhaei, F., Irannajad, M., 2017. Reagents types in flotation of iron oxide minerals: A review. Mineral Processing and Extractive Metallurgy Review 39 (2), 89–124. https://doi.org/10.1080/0882750 017.1391245.

Pavlovic, S., Brandão, P.R.G., 2003. Adsorption of starch, amylose, amylopectin and glucose monomer and their effect on the flotation of hematite and quartz. Minerals Engineering 16, 1117–1122.

Peres, A.E.C., Correa, M.I., 1996. Depression of iron oxides with corn starches. Minerals Engineering 9 (12), 1227–1234.

PubChem, 2020, Compound. Lauramidopropyldimethylamine. https://pubchem.ncbi.nlm.nih.gov/compound/lauramidopropyldimethylamine (Accessed 17th of December, 2020).

Severov, V.V., Filippova, I.V., Filippov, L.O., 2013. Floatability of Fe-bearing silicates in the presence of starch: adsorption and spectroscopic studies. J. Phys. Conf. Ser. https://doi.org/10.1088/1742-6596/416/1/012017.

Severov, V.V., Filippov, L.O., Filippova, I.V., 2016. Relationship between cation distribution with electrochemical and flotation properties of calcic amphiboles. Int J Mineral Processing 147, 18–27.

Smith, R.W., Scott, J.L., 1990. Mechanisms of dodecylamine flotation of quartz. Mineral Processing and Extractive Metallurgy Review 7 (2), 81–94. https://doi.org/10.1080/08827509008952667.

Turrer, H.D.G., Peres, A.E.C., 2010. Investigation on alternative depressants for iron ore flotation. Miner. Eng. 23, 1066–1069. https://doi.org/10.1016/j.mineng.2010.05.009.

Veloso, C.H., Filippov, L.O., Filippova, I.V., Ouvrard, S., Araujo, A.C., 2018. Investigation of the interaction mechanism of depressants in the reverse cationic flotation of complex iron ores. Minerals Engineering 125, 133–139.

Veloso, C.H., Filippov, L.O., Filippova, I.V., Ouvrard, S., Araujo, A.C., 2020. Adsorption of polymers onto iron oxides: Equilibrium isotherms. J Mater Res Technol 9 (1), 779–788.

Weissenborn, P., Warren, L., Dunn, J., 1995. Selective flocculation of ultrafine iron ore. 1. Mechanism of adsorption of starch onto hematite. Colloid. Surf. A: Physicochem. Eng. Asp. 99, 11–27. https://doi.org/10.1016/0927-7757(95)03111-P.

Xu, L., Hu, Y., Dong, F., Jiang, H., Wu, H., Zhen, W., Liu, R., 2015. Effects of particle size and chain length on flotation of quaternary ammonium salts onto kaolinite. Mineral. Petrol. 109, 309–316. https://doi.org/10.1007/s00710-014-0332-8.

Yuehua, H., Wei, S., Haipu, L., Xu, Z., 2004. Role of macromolecules in kaolinite flotation. Miner. Eng. 17, 1017–1022. https://doi.org/10.1016/j.mineng.2004.04.012.